



UPPSALA
UNIVERSITET

*Digital Comprehensive Summaries of Uppsala Dissertations
from the Faculty of Science and Technology 2153*

Micropatterning of hyaluronic acid hydrogels for *in vitro* models

ANA MARÍA PORRAS HERNÁNDEZ



ACTA
UNIVERSITATIS
UPSALIENSIS
UPPSALA
2022

ISSN 1651-6214
ISBN 978-91-513-1508-9
URN urn:nbn:se:uu:diva-473037

Dissertation presented at Uppsala University to be publicly examined in Sonja Lyttkens Hall (101121), Lägerhyddsvägen 1, Uppsala, Friday, 10 June 2022 at 21:44 for the degree of Doctor of Philosophy. The examination will be conducted in English. Faculty examiner: Professor Jörg Küttner (Copenhagen University).

Abstract

Porras Hernández, A. M. 2022. Micropatterning of hyaluronic acid hydrogels for *in vitro* models. *Digital Comprehensive Summaries of Uppsala Dissertations from the Faculty of Science and Technology* 2153. 80 pp. Uppsala: Acta Universitatis Upsaliensis. ISBN 978-91-513-1508-9.

The human body consist of a vast number of cells, and jointly, the cells, form tissues and organs. The cells interact and respond to their local microenvironment. The cellular microenvironment consists of a highly hydrated and compliant extracellular matrix, neighboring cells and circulating biochemical factors; and jointly, provide chemical and physical cues that regulate cell behaviour. However, these cues are often not present in traditional *in vitro* models, where cells experience a stiff and unstructured environment.

An approach to better mimic the *in vivo* microenvironment *in vitro* is to use hydrogels. Hydrogels are soft and highly hydrated polymers based on materials naturally found in the extracellular matrix of various tissues. Furthermore, these materials can be chemically functionalized to control the physical, chemical, and mechanical properties of the hydrogels. These functionalities can also be used to prepare micrometre sized cell adhesive regions, or micropatterns, on the hydrogel substrate. The micropatterns guide the cell shape and permit the study of the cell response to these changes in shape and function, which has been observed in e.g., endothelial cells from various origins.

Taken all together, the aim of this work was to develop a hydrogel-based cell culture substrate that permits the control of the spatial adhesion of brain endothelial cells in order to study the morphological effects on these cells and contribute to the understanding of the function of brain endothelial cells in health and disease.

This thesis demonstrates the functionalization of hyaluronic acid, a naturally occurring extracellular matrix polymer, to prepare photocrosslinkable hydrogels. Then, through photolithography, micropatterns of cell adhesive peptides were prepared on these hydrogels. Brain microvascular endothelial cells, a highly specialized type of endothelial cells, adhered to the micropatterns, and the effect on their alignment and cell chirality depending on the micropatterned sized was studied. Furthermore, changes in their alignment were also observed when exposed to different glucose concentration.

Keywords: Micropatterning, hyaluronic acid hydrogels, endothelial cells, alignment, cell chirality

Ana María Porras Hernández, Department of Materials Science and Engineering, Microsystems Technology, Box 35, Uppsala University, SE-751 03 Uppsala, Sweden.

© Ana María Porras Hernández 2022

ISSN 1651-6214

ISBN 978-91-513-1508-9

URN urn:nbn:se:uu:diva-473037 (<http://urn.kb.se/resolve?urn=urn:nbn:se:uu:diva-473037>)

To my family

List of Papers

This thesis is based on the following papers, which are referred to in the text by their Roman numerals.

- I A simplified approach to control cell adherence on biologically derived *in vitro* cell culture scaffolds by direct UV-mediated RGD linkage.
Porras Hernández, A. M., Pohlitz, H., Sjögren, F., Shi, L., Ossipov, D., Antfolk, M., Tenje, M.
Journal of Materials Science: Materials in Medicine 31:89 (2020)
Author's contributions: All experimental work. Major part of planning, evaluation, and writing.
- II Brain microvasculature endothelial cell orientation on micropatterned hydrogels is affected by glucose variation.
Porras Hernández, A. M., Barbe, L., Pohlitz, H., Tenje, M., Antfolk, M
Scientific Reports 11:19608 (2021)
Author's contributions: All experimental work. Part of planning, evaluation and writing.
- III Evaluation of cell chirality in brain microvascular endothelial cells.
Porras Hernández, A.M., Tenje, M., Antfolk, M.
Manuscript
Author's contributions: All experimental work. Major part of planning, evaluation, and writing
- IV A microfluidic chip carrier including temperature control and perfusion system for long-term cell imaging
Cantoni, F., Werr, G., Barbe, L., **Porras Hernández, A.M.**, Tenje, M.
HardwareX 10 (2021)
Author's contributions: Part of experimental work (on-chip staining protocol) and part of writing.

All papers are open access, distributed under the terms of the Creative Commons CC-BY license.

Other Work by the Author

A practical guide to microfabrication and patterning of hydrogels for biometric cell culture scaffolds.

Tenje, M.; Cantoni, F.; **Porras Hernández, A. M.**; Searle, S. S.; Johansson, S.; Barbe, L.; Antfolk, M.; Pohlitz, H.
Organs-on-a-Chip, 2:100003. (2020)

Author's contributions:

Major part of the writing of sections: *UV lithography* and *Chemical patterning of hydrogel scaffolds*.

Part of the writing of sections: *Soft lithography and moulding*, *Microfabricated cell-laden hydrogel constructs* and *Defined co-cultures from hydrogel modifications*.

Confocal imaging dataset to assess endothelial cell orientation during extreme glucose conditions.

Porras Hernández, A. M., Barbe, L., Pohlitz, H., Tenje, M., Antfolk, M.
Scientific Data 9:26 (2022)

Author's contributions: All experimental work and part of writing.

This thesis builds partly upon the author's licentiate thesis.

Chemical micropatterning of hyaluronic acid hydrogels for brain endothelial *in vitro* cell studies

Porras Hernández, A. M.

Uppsala University (2022)

From now on this is referred as licentiate thesis throughout this text.

The literature review has been reviewed and updated to fit in its new context. Of the papers included in this thesis, Paper I and II were part of the licentiate thesis. By chapters, the contribution from the licentiate thesis is as follows:

Introduction: This chapter was included in the licentiate thesis; for this thesis it has been reviewed and updated to fit in its new context. Around 10% of the text is new.

Chapter 1: This chapter was included in the licentiate thesis; around 20% of the text and references are new. Figure 1 is new.

Chapter 2: This chapter was included in the licentiate thesis; around 30% of the text and references are new. Figure 7 is new.

Chapter 3: This chapter was included in the licentiate thesis; around 30% of the text and references are new. Figures 12, 13 and 15 are new.

Chapter 4: This chapter was included in the licentiate thesis; around 10% of the text and references are new.

Chapter 5: This chapter was not included in the licentiate thesis.

Chapter 6: This chapter was included in the licentiate thesis; around 20% of the text and references are new. Figures 23 and 24 are new.

Chapter 7: This chapter was included in the licentiate; around 50% of the text is new.

Chapter 8: The summaries of Paper I and II (Chapter 8.1 and 8.2) were included in the licentiate. The text in Chapter 8.3 Summary of Paper III and 8.4 Summary of Paper IV is new. Figures 28 and 29 are new.

Contents

<i>Introduction</i>	<i>12</i>
<i>Chapter 1 Hydrogels for Cell Culture Scaffolds</i>	<i>14</i>
1.1 Hydrogels	15
1.2 Hyaluronic Acid Hydrogels	15
1.3 Crosslinking of Hyaluronic Acid Hydrogels	16
1.4 Hydrogel Mechanical Properties.....	17
<i>Chapter 2 Methods for the Microfabrication of HA-am Hydrogels for Cell Culture Scaffolds.....</i>	<i>19</i>
2.1 Photolithography	19
2.2 Micromoulding.....	21
2.2.1 Soft Lithography.....	21
2.2.2 Microcontact Printing.....	21
2.3. Other Fabrication Considerations	23
<i>Chapter 3 Controlling Cell Adhesion on HA-am Hydrogels.....</i>	<i>25</i>
3.1 Cell Adhesion.....	25
3.2 Controlling Cell Adhesion In Vitro	26
3.2.1 Micropatterning Methods	27
<i>Chapter 4 Microfabricated Brain Endothelial Cells In Vitro Models</i>	<i>32</i>
4. 1. Endothelial Cells and Brain Microvascular Endothelial Cells.....	32
4.2 General Considerations of the Study of Brain Endothelial Cells In Vitro	33
4.2.1 Cell Source	34
4.2.2 Cell Media	35
4.3 Glucose Effect on Brain Endothelial Cells	35
4.4 Endothelial Cells in Microfluidics Systems.....	36
4.5 Micropatterning of Endothelial Cells.....	37

<i>Chapter 5 Cell Chirality</i>	41
5.1 Study of Cell Chirality on Micropatterned Substrates	42
<i>Chapter 6 Analysis of Cell Morphology and Function In Vitro</i>	47
6.1 Immunofluorescence	47
6.2 Live Imaging	50
6.3 Fluorescent Microscopy	52
6.4 Image Analysis.....	53
<i>Chapter 7 Conclusions and Outlook</i>	56
<i>Chapter 8 Summary of Included Papers</i>	58
8.1 Summary of Paper I	58
8.2 Summary of Paper II	59
8.3 Summary of Paper III.....	61
8.4 Summary of Paper IV	62
<i>Popular Science Summary</i>	63
<i>Svensk Sammanfattning</i>	65
<i>Acknowledgements</i>	67
<i>References</i>	73

Abbreviations

2D	Two-dimensional
3D	Three-dimensional
bEnd.3	Mouse brain microvascular endothelial cell line
cAMP	Cyclic adenosine monophosphate
CCW	Counterclockwise
CW	Clockwise
Da	Daltons
E	Elastic modulus
ECM	Extracellular matrix
G	Shear modulus
G'	Storage modulus
HA	Hyaluronic acid
HA-am	Hyaluronic acid acrylamide
hCMEC/D3	Human cerebral endothelial cell line
HUVEC	Human umbilical vein endothelial cell
iPSC	Induced pluripotent stem cell
MEMS	Microelectromechanical systems
PDMS	Poly(dimethyl siloxane)
PEG	Poly(ethylene glycol)
PEGDA	Poly(ethylene glycol) diacrylate
PKC	Protein kinase C
RGD	Arginine-glycine-aspartic acid
UV	Ultraviolet
ν	Poisson's ratio of a material
VCAM-1	Vascular cell adhesion molecule-1
VEGF	Vascular endothelial growth factor
ZO-1	Zona occludens 1

Introduction

The human body consist of a vast number of cells, and jointly, the cells, form tissues and organs. Cells respond to their surroundings, or so-called microenvironment. The cell's microenvironment consist of a highly hydrated and compliant extracellular matrix, neighboring cells and circulating biochemical factors; that provide chemical and physical cues that regulate cell behaviour (1,2). However, these characteristics are often not present in traditional *in vitro* models used to study human physiology.

In vitro models consist of cells that are cultured outside their native environment. Cells are grown on a substrate that provides structural support for cell attachment and kept under a favourable artificial environment with defined and controlled experimental conditions. Traditional substrates for cell culture consist of a flat and stiff polystyrene plastic substrate. Polystyrene substrates offer a cheap and easy to use platform for *in vitro* studies, however, they lack the complex chemical and mechanical cues experienced by cells *in vivo*.

In recent years, there has been a great interest in the development and improvement of cell culture substrates for *in vitro* studies recapitulating the cell microenvironment. One of these approaches is the use of hydrogels, high water content polymers, that aim to mimic the native ECM (3,4). Through chemical modifications, polymers naturally found in the ECM, such as hyaluronic acid, can be functionalized to form crosslinked hydrogels. Moreover, these functionalities permit the modification of the hydrogels to present micrometre sized features that can guide cell behaviour. This has been achieved by using microfabrication techniques originally developed for the fabrication of electronic components(5).

Microfabrication techniques are a set of technologies that permit the construction of objects in the micrometre to millimetre range (6). Their use has permitted the formation of micropatterns on cell culture scaffolds to model the cell microenvironment *in vitro* (6,7). Micropatterns are micrometre sized cell adhesive regions on substrates (*e.g.* hydrogels) that impose a defined cell adhesion pattern and permit the study of morphological implications and effects on different cell types (8,9). For example, it has been demonstrated that endothelial cells increased their proliferation or apoptosis rates depending on the

size of the micropattern (10). Furthermore, micropatterning and it has contributed to the observation and study of cell chirality, an inherent property of involved in early tissue formation (10,11).

Endothelial cells line blood vessels throughout the body. Blood capillaries, or microvessels, participate in gas and nutrient exchange within tissues and form a barrier between the circulating blood and the underlying organ. Particularly, brain endothelial cells and present certain characteristics different to endothelial cells found in other organs, resulting in a particularly tight barrier (12,13). This barrier protects the brain harmful molecules and pathogens. However, it also impedes the passage of drugs treating diseases affecting the brain (14,15). Therefore, there is great interest in studying this endothelial cell subtype and has been the cell type of focus on this thesis.

Research Aim

Taken all together, the aim of this work is to:

1. Prepare a hyaluronic acid hydrogel cell culture scaffold
2. Control the spatial adhesion of brain endothelial cells
3. Study the morphological effects on these cells depending on the micropattern geometry
4. Explore the effect of varying glucose conditions on the cell's morphology
5. Explore the effect of the micropattern size on cell chirality

Chapter 1 Hydrogels for Cell Culture Scaffolds

Most cells *in vivo* are surrounded by an extracellular matrix (ECM). The ECM is composed of water, proteins, and polysaccharides. It provides biochemical and biomechanical cues and structural support to the cells, and ultimately give shape and structure to the tissue. Each tissue has a unique composition and mechanical properties (16). The stiffness of human tissue varies widely, as schematically summarized in **Figure 1**. On the other hand, *in vitro* studies utilize extensively polystyrene tissue culture plates as cell substrate, which have a stiffness of ~ 3.5 GPa, 1,000 times larger in magnitude compared to the e.g., brain stiffness (17). Furthermore, it has been widely observed that cells are responsive to the mechanical properties of their substrate *in vitro* (18,19).

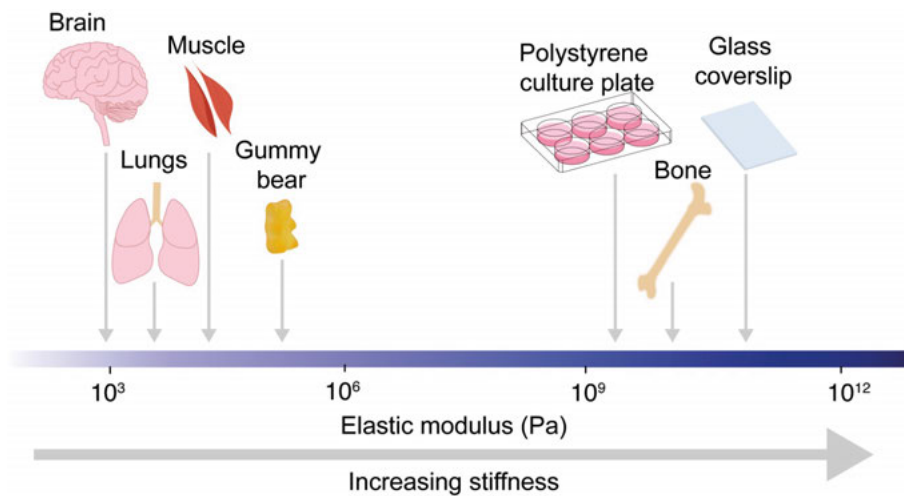


Figure 1. Schematic representation of the stiffness of various tissues and materials. Tissue stiffness is determined by their elastic modulus measured in pascals (Pa). Brain= ~ 1 kPa, lung= ~ 2 kPa, skeletal muscle= ~ 5 to 150 kPa, gummy bear= 60 kPa, tissue culture plate= ~ 3.5 GPa, bone= 20 GPa and glass= 70 GPa (17,19,20). The larger the elastic modulus the stiffer the tissue or material is.

Hydrogels have attracted interest to be used as cell culture substrates, due to their high-water content and similar mechanical properties as tissue *in vivo*. Moreover, hydrogel materials can be modified to present specific chemical,

mechanical and biological properties to better mimic the ECM of the desired tissue (3).

1.1 Hydrogels

Hydrogels are a type of materials that consist of crosslinked hydrophilic polymer chains, where water penetrates between the chains causing the swelling and formation of a hydrogel (3). Hydrogels can be formed by naturally derived or synthetic building blocks. Fibrin, collagen, and hyaluronic acid are naturally found in the ECM and have been used for preparation of hydrogels for cell culture. Alternatively, synthetic materials such as poly(ethylene glycol) (PEG) and polyacrylamide can be used (5,21). Most often, naturally derived materials are inherently cell adherent and can be used for cell culture without further modification. However, they are usually obtained from animal tissue and come with an inherent variability from batch to batch depending on the handling conditions. On the other hand, synthetic materials often require further functionalization to render cell adherent, however, they can offer greater control of the material properties (5,22).

1.2 Hyaluronic Acid Hydrogels

Hyaluronic acid (HA) is a naturally occurring glycosaminoglycan. HA is a linear polysaccharide consisting of alternating units of D-glucuronic acid and N-acetyl-D-glucosamine monosaccharides (**Figure 2**). It is negatively charged and attracts positive ions resulting in an osmotic balance that brings in water, resulting in a highly hydrated molecule (23). HA is one of the primary components of the ECM of different tissues throughout the body, including the brain (24). HA functions as a structural element in the ECM, maintaining a hydrated environment, modulating ion and molecule exchange and provide mechanical support for the cells. HA can interact with some cell surface receptors, being CD44 one of the most known and described (25).

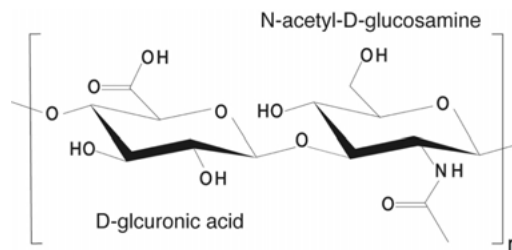


Figure 2. Hyaluronic acid. HA consists of alternating units of D-glucuronic acid and N-acetyl-D-glucosamine monosaccharides. Reproduced from licentiate thesis.

HA typically exists as high molecular weight (10,000 kDa) (26), but it can be cleaved by hyaluronidase, a cellular secreted enzyme, into lower molecular weight chains (27). Interestingly, high and low molecular weight HA have opposing effects on cell behaviour. High molecular weight (70 – 10,000 kDa) does not permit cell adhesion, while low molecular weight (~2.5 – 40 kDa) does (28,29). Therefore, HA further functionalization with cell adhesion motifs to be used as cell culture scaffold (23). However, this can be an advantage, as this opens the possibility of incorporating different cell adhesive molecules in a controlled manner. To take this a step further, one can spatially control the size and position of these molecules and add geometrical confinement into the system using microfabrication techniques to study their effect on cell adhesion (discussed further in Chapter 3).

1.3 Crosslinking of Hyaluronic Acid Hydrogels

Many of the materials used to form hydrogels are hydrophilic polymers, which might cause the hydrogel's dissolution over time under culture conditions (*i.e.*, in cell media). This can be prevented by forming chemically or physically crosslinked networks within the hydrogel (3). There are various crosslinking strategies, such as light, thermal, and ionic mediated (5). In this thesis a light mediated crosslinking (or photocrosslinkable) was used due to its compatibility with microfabrication techniques (discussed further on Chapter 2).

To prepare photocrosslinkable HA hydrogels, HA must be chemically functionalized to add reactive groups. HA contains functional groups along its backbone, where the carboxylic acid and hydroxyl groups are the two most commonly used groups for chemical modification (30). Photocrosslinkable HA hydrogels have been developed by functionalizing the HA backbone with different groups such as norbonene (31,32) and methacrylates (33–35).

In **Paper II** a photocrosslinkable HA derivative, hyaluronic acid acrylamide (HA-am) was prepared following a previously published protocol (36). In this manner, HA (MW= 135 kDa) was functionalized with acrylamide groups by reacting the carboxylic acid group of the HA backbone and the amino group of an aminoethyl acrylate linker, resulting in hyaluronic acid acrylamide (HA-am). Crosslinks will be formed between the acrylamide groups using UV light and a photoinitiator (**Figure 3**). Upon exposure to light, the photoinitiator absorbs photons and decomposes, forming free radicals. The radicals will then react with the vinyl bonds in the acrylamide groups causing the formation of chemical crosslinks between the polymer chains (9,37).

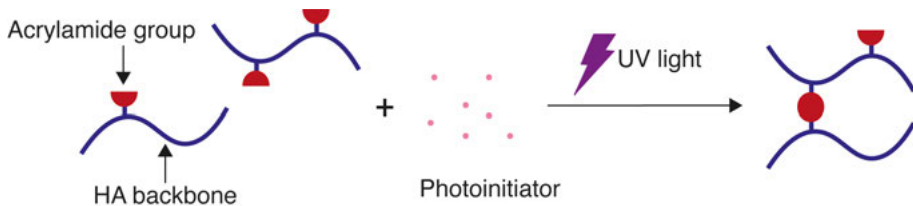


Figure 3. Photocrosslinkable hyaluronic acid acrylamide. Photocrosslinkable HA consists of HA functionalized with acrylamide groups. Upon UV light exposure the photoinitiator breaks down, forming radicals that will initiate the crosslinking between acrylamide groups. Reproduced from licentiate thesis.

Considerations for this type of crosslinking method are the type of photoinitiator, the photoinitiator concentration, and the exposure time. The photoinitiator type will determine the light wavelength. In this work, we used Irgacure 2959, one of the most common photoinitiators used due to its demonstrated compatibility to cells (37). Irgacure 2959 has an excitation wavelength between 320-390 nm (UV light) and this wavelength does not affect cellular DNA, compared to UV light used for sterilization (240-280 nm). The photoinitiator concentration must be chosen carefully and determined experimentally as it will affect the crosslinking degree. Too high or too low photoinitiator concentration will lead to too slow or too fast polymerization respectively, resulting in a weak hydrogel (38). Finally, the exposure time (*i.e.* reaction time) will determine the degree of crosslinking. This in turn will affect the mechanical properties of the hydrogel which will be discussed in the following section.

1.4 Hydrogel Mechanical Properties

One of the main features and interest of using hydrogels for cell culture is that their stiffness is closer to tissue *in vivo* compared to cell culture polystyrene. The stiffness of a material is described by its elastic modulus (or Young's modulus, E) or their shear modulus (G). The hydrogel's elastic modulus is a measure of the strain when stress is applied to a material, *i.e.*, it describes the extent of deformation (strain) due to an applied force (stress). The shear modulus describes this ratio, when shear forces are applied to the material (39). G and E are related as shown by the equation $E = 2G(1 + \nu)$; where ν is the material's Poisson's ratio (21). HA hydrogels, and most hydrogels, have a Poisson's ratio of ~ 0.5 (21,31,40), therefore this relation approaches $E \approx 3G$.

G can be determined by experimental techniques such as shear rheometry. In shear rheometry measurements, the crosslinked hydrogel is placed between two plates and a constant strain is applied to the material in a range of frequencies (Figure 4). These measurements provide the storage (G') modulus, which

represents the energy stored during material deformation, describing the elastic behaviour of the material (39). To determine and compare the mechanical properties of different hydrogels, the G' from a selected frequency in the linear region was used to calculate E , using the above approximation, where $G' \approx G$.

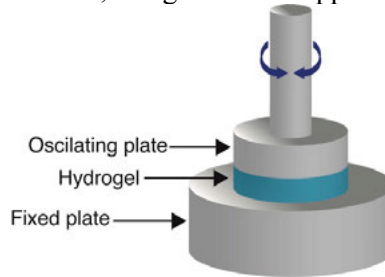


Figure 4. Shear rheometry. The hydrogel is placed between a fixed plate and an oscillating plate. The oscillation is applied at a fixed strain. Reproduced from licentiate thesis.

The stiffness of HA hydrogels can be varied by controlling the degree of cross-linking in the hydrogel. In the case of UV crosslinkable HA hydrogels this can be controlled by increasing or decreasing the UV exposure time. As a rule of thumb, longer UV exposure times will result in stiffer hydrogels (32,33). Another approach is to increase the concentration of HA in the precursor solution, where increasing the HA concentration will result in an increased stiffness (23). Photocrosslinkable HA hydrogels have been reported to have an elastic modulus from 0.51 kPa up to 100 kPa (32,35). Hydrogels can have stiffness values within kPa range and do therefore provide a more biomimetic environment for culturing cells *in vitro*.

Chapter 2 Methods for the Microfabrication of HA-am Hydrogels for Cell Culture Scaffolds

Photocrosslinkable hydrogels are an interesting material as cell culture scaffold, not only due to their tunability to better mimic the mechanical properties of tissue *in vivo*, but also due to their compatibility with microfabrication techniques.

Microfabrication is a set of technologies that permit the construction of objects in the micrometre to millimetre range, such as microelectromechanical systems (MEMS) (6). The fabrication of MEMS relies widely on photolithography, and it is often the first step in the fabrication process. Even, micromoulding and soft lithography, rely in photolithography. These microfabrication techniques have now been extensively used in the development of various tools to study biological systems, a field often referred to as BioMEMS (7).

In this section, the basics of different microfabrication techniques, that have been used for the microfabrication of hydrogels, will be introduced. Then, how these methods have been adapted for the microfabrication of 2D and 3D structures in hydrogels for cell culture scaffolds will be discussed.

2.1 Photolithography

Photolithography is one of the most important techniques, and commonly the starting point in the fabrication of MEMS (7). This technique permits the fabrication of micrometre sized 3D structures on a substrate. This method consists in preparing a thin uniform film of a photosensitive material (photoresist) on a substrate, *e.g.*, silicon wafer. The photoresist is then covered with a photo-mask, with the desired microscale pattern, that will protect or expose some regions to UV light. UV exposure will cause chemical changes on the photoresist and modify its solubility in a developer solution. Photoresists can be negative or positive, where a positive resist becomes soluble when exposed to UV light and a negative photoresist becomes insoluble (**Figure 5**). SU-8 is a negative photoresist widely used to fabricate chips and master moulds (41).

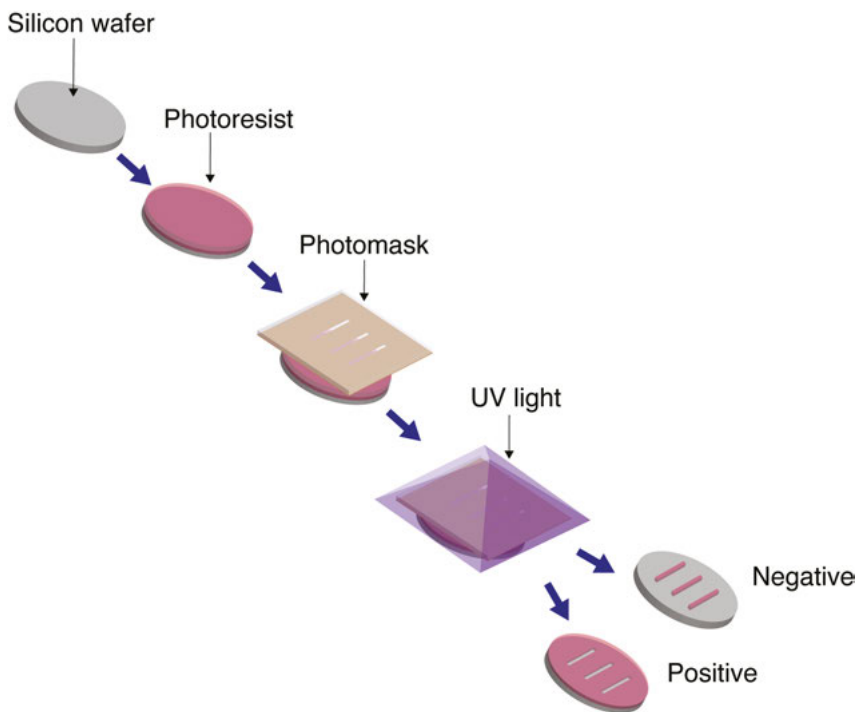


Figure 5. Photolithography. A photoresist film is deposited on a silicon wafer. The photoresist is then covered with a photomask containing the desired micrometre features. Then, the photoresist is exposed to UV light through the photomask opening. The resulting structure will depend on the photoresist properties. The photoresist can be negative or positive. A positive resist becomes soluble when exposed to UV light. A negative photoresist becomes insoluble after UV light exposure. Adapted from licentiate thesis.

Using this technique, it is possible to fabricate small structures with high resolution. Resolution refers to the smallest structure size that can be achieved. It depends on various parameters in the process, such as the material being patterned (*e.g.*, SU-8, hydrogel, peptide, protein), the substrate being patterned (*e.g.*, silicon, glass, hydrogel) and the photomask. Photomasks can be made on glass or plastic films. For high resolution applications ($\sim 1\ \mu\text{m}$ sized structures), chrome-glass photomasks are required. For lower resolution requirements, the mask can be prepared by toner ink printed on transparency films ($\sim 50\ \mu\text{m}$). Overall, the required and achievable resolution is application dependent (7).

Photocrosslinkable hydrogels can be processed using photolithography to form 3D structures (5,42). The process is very similar to silicon-based lithography, where the photoresist is the hydrogel. HA-am hydrogels can be compared to a negative photoresist, *i.e.*, the hydrogel is activated and forms

crosslinks when exposed to UV light and becomes insoluble in water, while the non-exposed areas will dissolve. 2D micropatterns can also be formed on the hydrogel surface using the same approach which will be discussed further in Chapter 3.

2.2 Micromoulding

Micromoulding is an important set of methods for the microfabrication of materials that cannot be patterned using photolithography. It is particularly useful for shaping polymer materials once a master mould is fabricated. Moulds with micrometre sized features can be fabricated by photolithography, for example using SU-8 on silicon. This method is widely used for soft polymers, specifically poly(dimethylsiloxane) (PDMS), resulting in soft lithography, a subfamily of micromoulding with extensive use in BioMEMS (7).

2.2.1 Soft Lithography

Soft lithography consists in the use of a micromolded piece of PDMS to create a pattern or form a device, *e.g.*, microfluidic device (**Figure 6**). PDMS is an elastomeric polymer, with physicochemical properties that are advantageous for BioMEMS, such as soft, optically transparent, biocompatible and permeable to gases. PDMS is thermally cured by first mixing the PDMS pre-polymer (monomer) and a crosslinking agent. The mixture is then poured over the master mould and let to solidify. Once cured, the micromoulded PDMS piece can be peeled off from the mould and the mould can be reused (7).

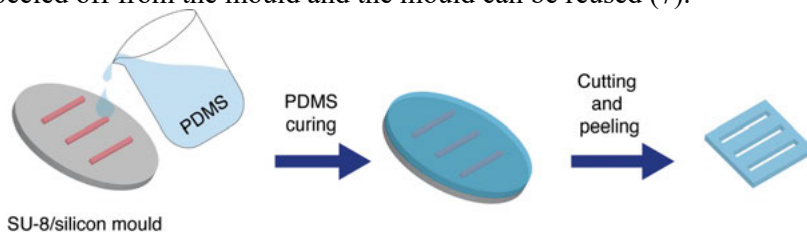


Figure 6. Soft lithography. A mixture of PDMS pre-polymer and crosslinking agent is poured in the silicon master mould and the PDMS is left for curing. After the cross-linked solidified PDMS can be removed or peeled off the master mould and cut to the desire size and shape. After, the master mould can be reused to replicate the pattern. Reproduced from licentiate thesis.

2.2.2 Microcontact Printing

This method consists of the transfer of a molecule of interest from a microfabricated piece of PDMS, *i.e.*, stamp, onto a surface. The PDMS contains the micrometre sized pattern. The molecule will then transfer only on the areas

contacted by the stamp (7) (**Figure 7**). This technique mostly works for formation of 2D patterns on a stiff substrate. However, it has been adapted to pattern hydrogels and will be discussed further in Chapter 3.

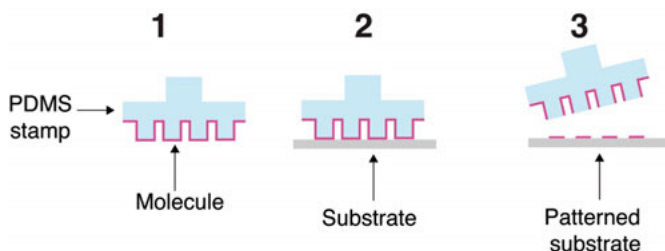


Figure 7. Microcontact printing. (1) This method consists in the transfer of a molecule from a PDMS stamp to a substrate. (2) The stamp is placed in contact with the substrate to pattern. (3) The molecule will be transferred only to the areas that were in contact with the stamp.

Micromoulding is very useful in shaping hydrogel precursors during cross-linking. Hydrogel precursors are dissolved in a buffer solution and then cross-linked by different means (*e.g.*, exposure to light or a temperature change). In this manner, hydrogels can be formed in specific shapes in moulds. In Paper I, II and III, HA-am hydrogels were micromolded using a silicon/SU-8 mould on a glass substrate, resulting in an 8 mm in diameter and 200 μm thick structure (**Figure 8**).

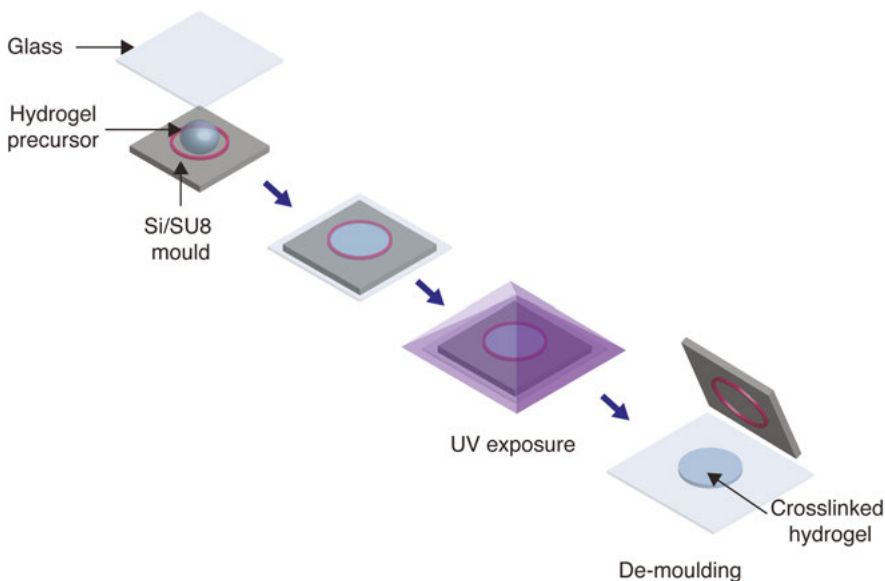


Figure 8. Micromolded hydrogel. Hydrogels can be crosslinked inside a silicon/SU-8 micromould. First the prepolymer solution is placed inside the mould and covered by a glass coverslip. Then, the hydrogel precursor is exposed to UV light through the glass. Finally, the mould is removed, and the crosslinked hydrogel with the shape of the mould remains on the glass. Adapted from licentiate thesis.

2.3. Other Fabrication Considerations

Hydrogels are soft materials, and their handling can be difficult. Hydrogels used for cell culture might need to undergo many processing steps such as micropatterning, cell culture and microscopy imaging. Moreover, during the cell culture the gel is submerged in cell media, usually by placing the hydrogel inside well plates, where the hydrogel might float. This will cause problems in seeding cells and microscopy to keep track of the culture. Moreover, *in situ* analysis of cells growing on the hydrogel is often desired using immunofluorescence techniques and confocal microscopy (discussed further in Chapter 5). To this end, hydrogels can be fabricated on glass coverslips to allow easy handling of the hydrogel during these steps.

Glass is a good support material due to its compatibility with confocal microscopy and biocompatibility in cell studies. Glass silanization permits covalent attachment of the hydrogel onto the coverslip (21). Silanization is the deposition of silanes onto substrates. Silanes are chemical compounds with a central silicon atom and contain two reactive groups (**Figure 9A**), one that will react with hydroxyl groups present on the glass substrate (X in **Figure 9A**), and a second one that will bind covalently to the hydrogel (R in **Figure 9A**) (43,44).

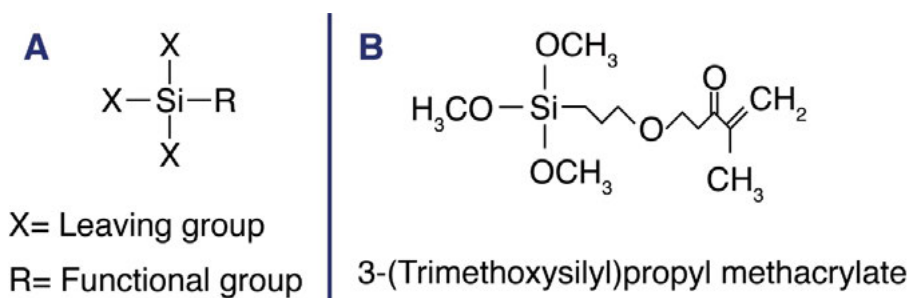


Figure 9. Silanes. A. Silanes are chemical compounds formed by a central silicon atom with four attachments, consisting of a functional group (R) and leaving groups (X). B. Chemical formula of silane methacrylate (3-(trimethoxysilyl)propyl methacrylate). Adapted with permission by Elsevier. Ratner, B. D., & Hoffman, A. S. Physicochemical surface modification of materials used in medicine. (pp. 259-275) Copyright 2013. Reproduced from licentiate thesis.

This approach was used in the design and development of the cell culture scaffolds in Papers I - III. For this purpose, 175 μm thick glass was functionalized with silane methacrylate (3-(trimethoxysilyl)propyl methacrylate) (**Figure 9B**). In this manner it was possible to micro-mould and attach a HA-am hydrogel on a glass substrate, which could be further handled for 2D patterning, followed by cell culture. Later, this treatment permitted the handling of the hydrogel with cells going through immunofluorescence processing, sustaining multiple washes and finally confocal imaging and long-term storage.

Chapter 3 Controlling Cell Adhesion on HA-am Hydrogels

In traditional cell culture substrates, *i.e.*, polystyrene plates, cell adhesion is mediated by adsorbed proteins on the polystyrene substrate present in the cell medium (45,46). *In vivo*, cells are exposed to a highly structured ECM and neighbouring cells that impose boundary conditions that dictate the cell architecture. These conditions are not achieved in traditional cell culture substrates, where cells are rather exposed to homogenous and unstructured cell adhesive substrate (8).

As previously mentioned, HA hydrogels are mostly synthesized from high molecular weight HA and requires its further functionalization with cell adhesion motifs to be used as cell culture scaffold (23). However, this can be an advantage, as this opens up the possibility of incorporating different cell adhesive molecules in a controlled manner. To take this a step further, one can spatially control the size and position of these molecules and add geometrical confinement into the system using microfabrication techniques to study their effect on cell adhesion. Microfabrication techniques has permitted the spatial control of chemical functionalities, to control the appearance of cell adhesive regions, or micropatterns, on various substrates, including hydrogel materials.

3.1 Cell Adhesion

Cells attach to a substrate (ECM or polystyrene plate) through the process of cell adhesion mediated by integrins (47). Integrins are transmembrane proteins that interact with ECM proteins, mediating cell attachment and signal transduction inside the cell (**Figure 10**). Moreover, integrins also bind to the cytoskeleton, through actin binding proteins and stabilizes the cell-matrix interactions. Integrins are heterodimeric proteins consisting of a large extracellular domain and a short cytoplasmic domain. There have been identified 24 different heterodimers in mammalian cells (48). Usually, individual cell types express multiple integrins, and each integrin can bind to various proteins and vice versa. Fibronectin, collagen and laminin are some of the proteins present in the ECM that are ligands for integrins (47,48).

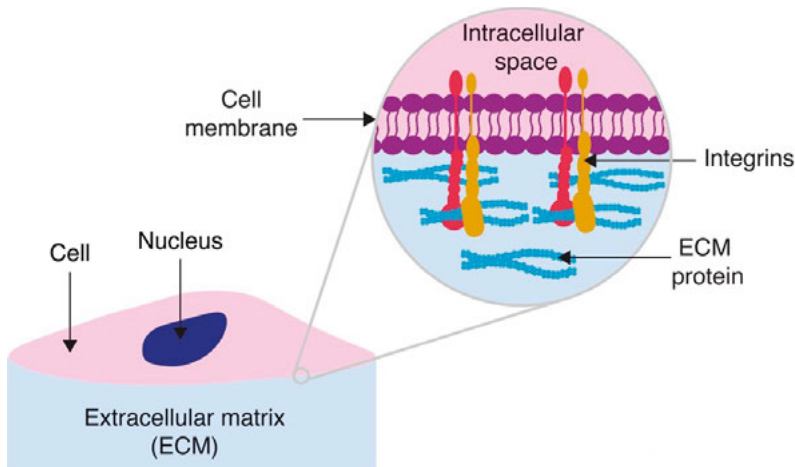


Figure 10. Integrin mediated cell adhesion. Integrins are heterodimeric proteins found in the cell membrane. They bind to proteins found in the extracellular matrix, mediating cell adhesion. Adapted from licentiate thesis.

There is a wide variety of integrins and integrin ligands, and several integrin-ligand combinations have been identified. Moreover, it has been shown that integrins bind to short amino acid sequences on the proteins. The RGD peptide sequence (arginine-glycine-aspartic acid) is one of the minimal integrin recognition sequence found in fibronectin, vitronectin and fibrinogen; and about one third of the integrins bind to this sequence (48,49).

3.2 Controlling Cell Adhesion In Vitro

Micropatterns are micrometre sized cell adhesive regions on otherwise non-cell adhesive substrate. Micropatterns can vary in shape and size, resulting in the geometrical confinement of cells (8,9). Upon cell adhesion, the cells adapt their shape and their cytoskeletal actin filaments to the underlying micropattern, as shown in **Figure 11** (50).

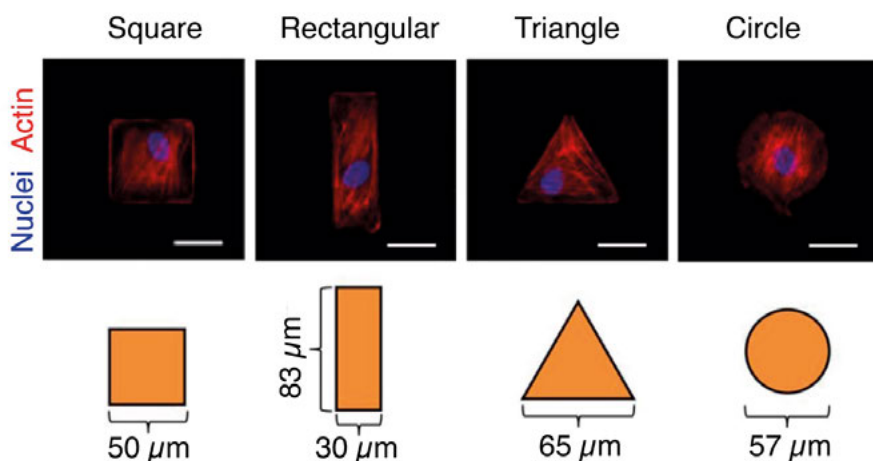


Figure 11. Micropatterning cells. Cells adapt their shape to the underlying pattern. Single human umbilical vein endothelial cells (HUVECs) seeded on fibronectin micropatterns of various geometries with a constant cell adhesive area of $2500 \mu\text{m}^2$. Scale bars: $30 \mu\text{m}$. Adapted with permission of Journal of Cell Science. Florian A. Gegenfurtner, Berenice Jahn, Helga Wagner, Christoph Ziegenhain, Wolfgang Enard, Ludwig Geistlinger, Joachim O. Rädler, Angelika M. Vollmar, Stefan Zahler; Micropatterning as a tool to identify regulatory triggers and kinetics of actin-mediated endothelial mechanosensing. *J Cell Sci* 15 May 2018; 131 (10): jcs212886. Reproduced from licentiate thesis.

In order to covalently link adhesive molecules on the surface of the substrate, the molecule to be patterned must contain chemical groups that can react with the substrate. Micropatterns can consist of full proteins or short peptide sequences that integrins recognize and bind to. Peptides are inexpensive and less sensitive to denaturation, compared to full proteins. Furthermore, they are easy to synthesize, and it is possible to design specific peptide sequences that might be required.

3.2.1 Micropatterning Methods

Micropatterns can be prepared on a variety of substrates, such as glass, polystyrene culture plates and hydrogels. The first examples of micropatterning were prepared using microcontact printing on glass substrate (51). Later, advances in biomaterials functionalization, specifically the functionalization of hydrogels with reactive groups, and their combination with microfabrication has opened up the opportunity to prepare micropatterns on more compliant materials.

3.2.1.1 Microcontact Printing

Microcontact printing has been widely used to prepare 2D micropatterns on stiff substrates such as glass. This method requires a PDMS stamp with the desired pattern fabricated via soft lithography (as discussed in Chapter 2). The first examples of micropatterning for controlling the shape and position of cells were prepared using microcontact printing. Briefly, a cell adhesive molecule, usually a protein as fibronectin, is inked to the PDMS stamp. Then the PDMS stamp is placed in contact with the substrate, generally glass. Then the protein is transferred only to the areas where the PDMS stamp was in contact with (Figure 12).

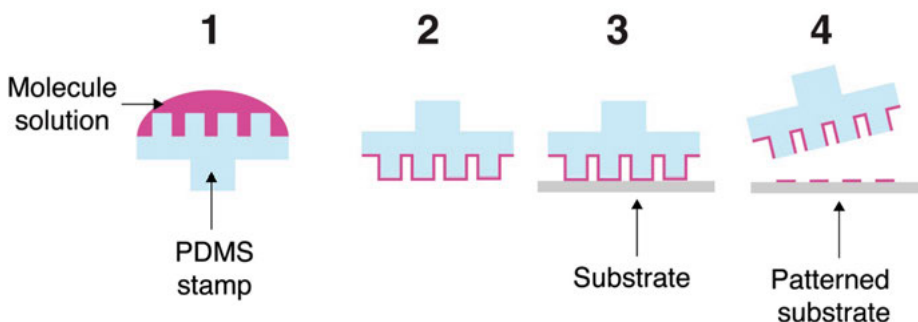


Figure 12. Microcontact printing of cell adhesive molecules on a substrate. (1) Inking of PDMS stamp. (2) Inked stamp. (3) Printing on desired substrate (4) Resulting patterned substrate.

Microcontact printing is not the first choice the patterning of hydrogels due to the soft nature of the hydrogels and the requirement of certain amount of force during microcontact printing, resulting in structural damage and loss of integrity of the hydrogel. However, some approaches have been developed to overcome these problems. For example, by forming a hydrogel layer and freeze dry it. Then the freeze-dried hydrogel has the stability to sustain a microcontact printing step (52). Another approach consists in first depositing the cell adhesive molecule on a solid substrate (*e.g.*, glass) following the standard microcontact printing steps (Figure 12). Then the adhesive molecule is transferred from the solid substrate to the hydrogel, by placing the hydrogel precursor solution and leave it to crosslink while the adhesive molecule is transferred, as depicted in Figure 13 (5,53). Overall, while these methods have successfully patterned hydrogels for cell culture scaffolds, these approaches add complexity to the process and are time consuming.

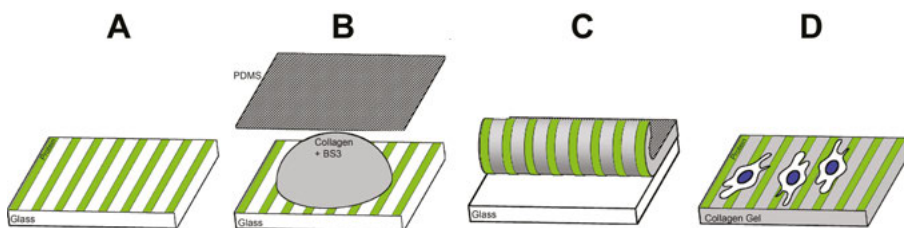


Figure 13. 2D patterning of collagen hydrogels via microcontact printing. **A.** Glass substrate with patterned molecule, prepared via microcontact printing. **B.** The uncross linked collagen hydrogel is placed on the patterned glass. The hydrogel is pressed with a PDMS sheet to form a uniform layer and left to crosslink while the pattern is transferred. **C.** Peeling off the crosslinked patterned hydrogel. **D.** Cell seeding on patterned hydrogel. Adapted from *Biomaterials*, 39, Hsiao, T. W., Tresco, P. A. & Hlady, V. Astrocytes alignment and reactivity on collagen hydrogels patterned with ECM proteins, 124-130, Copyright 2015, with permission from Elsevier.

3.2.1.2 Photolithography

Photolithography has been widely used for the preparation of 2D patterns on hydrogel substrates. Photolithography is preferred for micropatterning of hydrogels since it is mechanically gentler than microcontact printing. One of the first examples of micropatterning hydrogels was shown by Hanh et al., where poly(ethylene glycol) diacrylate (PEGDA) hydrogels were patterned with RGD peptides functionalized with PEGDA (54).

In Paper I, a simplified approach to prepare and micropatterned hyaluronic acid hydrogels was developed (**Figure 14**). In this method, a cysteine containing RGD peptides (GCGYRGDSPG) was patterned on the surface of micromolded HA-am hydrogels using photolithography. First the hydrogel is covered with an RGD peptide solution, covered with a photomask with the desired pattern and exposed to UV light. The photoinitiator molecules in the exposed regions will break and form radicals, initiating thiol-ene reactions between the thiol group in the peptide and the acrylamide on the HA-am backbone.

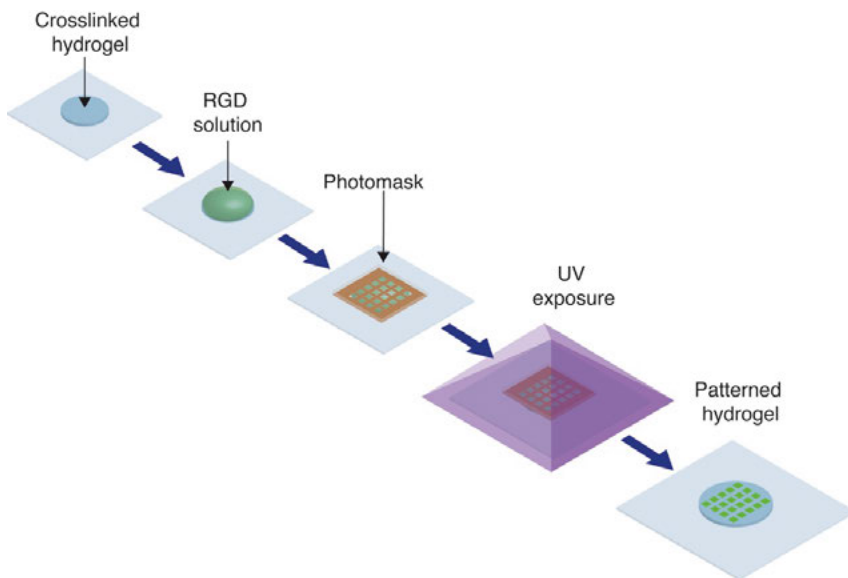


Figure 14. Photopatterning HA-am hydrogels with RGD peptides. First, a thiol containing RGD peptide solution is placed on top of the micromolded crosslinked hydrogel. Then, a photomask is placed in close contact to the peptide solution and hydrogel with the desired pattern. The system is then exposed to UV light, where the photoinitiator molecules in the exposed regions will break and form radicals, initiating thiol-ene reactions between the thiol group in the peptide and the acrylamide on the HA-am backbone. Adapted from licentiate thesis.

In this method, a cysteine containing RGD peptides (GCGYRGDSPG) were used. The cysteine contains a thiol group (SH) that can react with the acrylamide groups on HA-am, via so-called thiol-ene reactions (**Figure 15**). Thiol-ene reactions occur between a thiol and an alkene group. Alkenes are hydrocarbons containing a carbon – carbon double bond. Thiols present weak sulphur hydrogen bonds and can be broken under mild conditions (55). Thiol-ene reactions can be initiated by free radicals, *i.e.* requires an initiator to generate radicals that will initiate the reaction. This can be achieved with photoinitiators, and naturally Irgacure 2959 can be used. Furthermore, it is possible to control the amount of peptides attaching to the hydrogel substrate, where longer UV exposure result in more amounts of peptides attaching to the hydrogel, as demonstrated in **Paper I**.

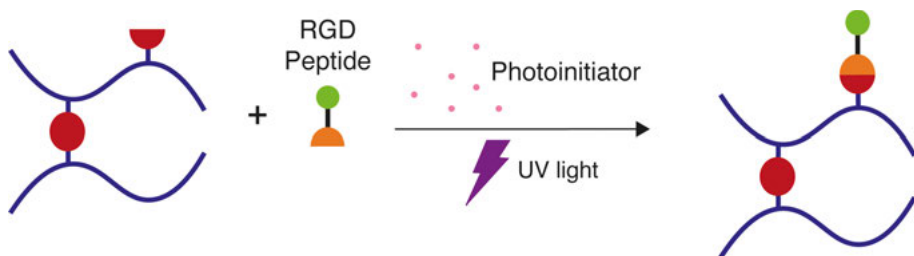


Figure 15. Schematic of photoinitiated thiol-ene reaction. The thiol-ene reactions occurs between the alkene and thiol group. The alkene group is present in the acrylamide group (depicted in red) in HA-am. The thiol group (depicted in orange) is present in the RGD peptide sequence, in a cysteine peptide. The reaction is initiated by a photoinitiator which decomposes and form radicals upon UV exposure.

The use of micropatterns have permitted the study the morphological implications and effects on different cell types (8), including endothelial cells from various origins (56) and it will be discussed further on the following chapter (Chapter 4).

Chapter 4 Microfabricated Brain Endothelial Cells *In Vitro* Models

Endothelial cells line the blood vessels in our bodies and their phenotype vary between the vessel type and the organ they vascularize, exhibiting differences in cell morphology, function and gene expression (12,57,58). Brain microvascular endothelial cells are a type of highly impermeable endothelial cells that protect the brain by forming the so-called blood-brain barrier.

Two particular microfabrication techniques that have been adopted for the study of endothelial cells *in vitro* are micropatterned substrates and microfluidic systems. Micropatterned models have provided mechanistic information on the effect on the morphology of endothelial cells (56). Moreover, microfluidic systems have been used to emulate blood flow *in vitro* and have provided insightful information about the function of endothelial cells (59) and for this reason they will also be discussed briefly in this section.

4. 1. Endothelial Cells and Brain Microvascular Endothelial Cells

Blood vessels deliver blood containing oxygen and nutrients to the tissues and remove carbon dioxide and metabolic waste. Arteries deliver oxygenated blood to the tissue, while veins drain the deoxygenated blood. Blood capillaries, or microvessels, participate in gas and nutrient exchange within tissues and are much smaller, $\sim 10\text{ }\mu\text{m}$ in diameter, compared to veins and arteries (12,13,57,58,60).

The blood capillaries of the brain constitute a barrier between the brain and the rest of the body known as the blood-brain barrier. The blood-brain barrier consists of a microvessel network, formed by brain microvascular endothelial cells, surrounded by a basement membrane, pericytes, astrocytes end-feet (**Figure 16**). The blood-brain barrier tightly modulates the movement of molecules, ions and cells between the blood and the brain, while it also protects the brain from the passage of toxins and pathogens. However, this restrictive behaviour is also an obstacle for drug delivery to the brain (13). While the function of brain microvascular endothelial cells is influenced by pericytes

and astrocytes, it is the brain microvascular endothelial cells that form the physical and structural basis of the barrier. Moreover, they exhibit a highly specialized phenotype, compared to other endothelial cells, and this thesis has focused on the study of this subtype.

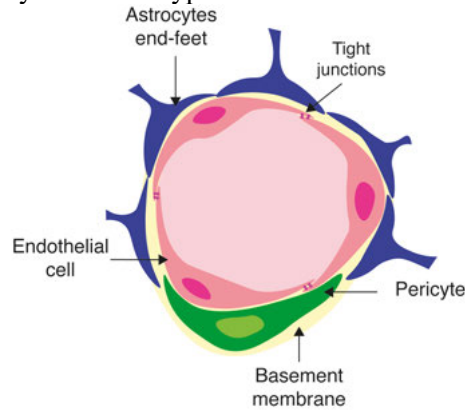


Figure 16. The blood brain barrier. The blood brain barrier is formed by endothelial cells lining the blood capillaries. The endothelial cells are surrounded by a basement membrane, pericytes and astrocytes end-feet. Reproduced from licentiate thesis.

Brain microvascular endothelial cells are non-fenestrated, *i.e.*, they lack trans-cellular pores, present in other endothelial cells. Moreover, they are particularly rich in tight junctions, conferring the blood-brain barrier decreased permeability. Claudins, occludins and junction adhesion molecules are tight junction proteins that have been identified in contributing to blood-brain barrier tightness. Tight junctions are transmembrane proteins that bind to each other between adjacent cells, and to their respective cell to actin fibres through tight junction accessory proteins, such as zona occludens 1 (ZO-1) (13,57,58,61).

4.2 General Considerations of the Study of Brain Endothelial Cells In Vitro

In vitro models facilitate the study of specific parameters to understand changes governing the endothelial cell's function. These studies consist in growing cells outside their native tissue. Naturally, the selection of parameters, such as cell source and growth conditions (substrate and medium) will have a great effect in the outcome of the study and must be chosen carefully, depending on the aim of the study.

4.2.1 Cell Source

Brain microvascular endothelial cells can be obtained from various sources. For example, they can be directly from a brain tissue section which is disaggregated and then cells are isolated to be cultured. However, the recovery of the specific cell type can be challenging, and primary cultures are often contaminated with other cell types, such as pericytes. Primary mature cells have a limited life span, due to senescence, a genetically determined loss of proliferative behaviour and can only be used for ~ 6 passage and they can also undergo de-differentiation overtime. Another challenge is the access to human brain tissue to obtain primary brain endothelial cells and for this reason often primary cells are obtained from animal tissue (62).

Another source of endothelial cells for *in vitro* studies are immortalized cell lines. Commonly used immortalized brain endothelial cells are hCMEC/D3 (human) and bEnd.3 (mouse). These cell lines are primary cultures that have been immortalized, by blocking inhibition of cell cycle progression, using viral genes (62). Cell lines can be used for up to 40 passages, depending on the cell line, which is a great advantage over primary cells.

Stem cells are another source of cells for *in vitro* studies. Stem cell can differentiate into more mature and specialized cell types. Stem cells can be categorized into two main groups, adult, and pluripotent stem cells, based on their differentiation potential. Adult stem cells, non-embryonic or somatic stem cells, are found in tissues and organs; and can differentiate into specialized cell types of that tissue or organ. Pluripotent stem cells, embryonic stem cells and induced pluripotent stem cells (iPSCs), can differentiate into all types of cells found in the body. iPSCs are originally mature adult cells that are reprogrammed into pluripotent embryonic stem-like state (63). Moreover, they can be propagated extensively and obtained from clones (64). iPSCs are particularly useful when the access to embryonic stem cells is limited.

Immortalized cell lines are well characterized, they are readily available and are easy to maintain, compared to stem cells and primary cells. However, they can present altered expression of tight junction proteins that are characteristic of brain microvascular endothelial cells (65–67). However, they are a viable alternative and have been widely used for *in vitro* studies of brain endothelial cell's function. Moreover, they are a cost-effective alternative, particularly for the development of cell culture scaffolds (67).

4.2.2 Cell Media

The cell medium is a defined mixture of a source of energy, nutrients, salts, and amino acids. Glucose is the common energy source found in cell media and a normal amount of glucose in media is 5.5 mM. However, different glucose concentrations affect cell function, for example, the amount of glucose might be increased to 25 mM to keep high proliferation rates during cell culture maintenance. On the other hand, increasing glucose concentration can also have negative effects on brain microvascular endothelial cells, including bEnd.3 cells (68–70). For example, it has been reported that 25 mM glucose increases apoptosis rates in bEnd.3 cells, compared to cells exposed to 5 mM glucose concentration for 48h (68).

Glucose variation in cell media can be used to study diabetes *in vitro* to determine the underlying mechanisms in glucose and endothelial cells dysfunction. Glucose concentration can be increased between 25 to 35 mM to mimic hyperglycaemia, decreased to 1 to ~ 2.2 mM to mimic the hypoglycaemic case, while 5.5 mM glucose concentration represents healthy homeostasis (68,70–73). In this line, various studies have been performed on brain endothelial cells to study the effect of glucose on cell function and will be discussed briefly in the following section.

4.3 Glucose Effect on Brain Endothelial Cells

It has been observed in human and animal studies, that diabetes mellitus affects blood-brain barrier permeability (74–76). However, the mechanisms of how the blood-brain barrier is involved in diabetes mellitus are still not completely well understood (74,75). In the following section, *in vitro* studies on the effect of extreme glucose levels on brain endothelial cells, will be briefly presented, with particular focus of studies using bEnd.3 cells, as this is the cell line used in this thesis.

It has been shown that bEnd.3 cells display a decrease in viability after 48h, but not after 24h of 25 mM and 40 mM glucose exposure (70). Permeability studies have also demonstrated that exposure to high glucose (30 and 50 mM) concentrations increases permeability of bEnd.3 cells, in a time (1, 3, 6 and 10 days) and dose dependent manner, compared to normal glucose level conditions (5.5 mM). This increased permeability was accompanied by decreased expression of ZO-1 and occludin, while claudin-5 expression was not affected. Furthermore, ZO-1 and occludin arrangement was altered, *i.e.*, discontinuous (69). On the other hand, the permeability of bEnd.3 cells exposed to hypoglycaemic conditions (0.5 and 1 mM) was increased in a time (6, 12 or 24h) and dose dependent manner, where greater permeability was observed on bEnd.3

cells exposed to 0.5 mM glucose for 24 h. Interestingly, hypoglycaemia did not affect the expression of ZO-1 and occludin, but claudin-5 expression decreased (73).

Changes in permeability and tight junction protein expression have also been observed on other brain endothelial cells cell lines. For example, hCMEC/D3 cells showed downregulation of ZO-1 and claudin-5 hypoglycaemic (2.2 mM), while no effect was observed on the protein expression under hyperglycaemic conditions (35 mM). However, ZO-1 was discontinuous at the cell-cell contacts. Furthermore, increased permeability was observed under both hypoglycaemic and hyperglycaemic conditions (72). Moreover, endothelial cells alignment has been affected due to variations in glucose level in the media on microfluidic devices and on micropatterned systems which will be discussed further in the following sections.

4.4 Endothelial Cells in Microfluidics Systems

Endothelial cells align to the direction of the blood flow and present an elongated cell morphology corresponding to a healthy, atheroprotective phenotype (56,77). Microfluidic systems, fabricated via soft lithography, have been used to simulate the blood flow that endothelial cells experience *in vivo* (59).

Microfluidic devices can be fabricated using soft lithography. In their most basic configuration, they consist of a microfluidic channel in PDMS bonded to a glass substrate. The PDMS piece also contains inlet and outlet openings for the flow of cell media. Microfluidic devices offer precise control over the media flow to model different regiments of blood flow, experienced by endothelial cells depending on the type of blood vessel they line. Furthermore, they minimize the amount of cells, media and reagents necessary for their culture and their assessment of function.

It has been observed that human umbilical vein endothelial cells (HUVECs) align to the direction of the flow in microfluidic devices. Their nuclei and actin filaments re-organize and follow the direction of the flow (71,78,79). However, endothelial cells responses to flow *in vitro* have been different depending on the endothelial cell origin, where brain endothelial cells do not align to the direction of the flow. This has been observed on immortalized human brain endothelial cells (80) and on iPSC-derived brain endothelial cells (81).

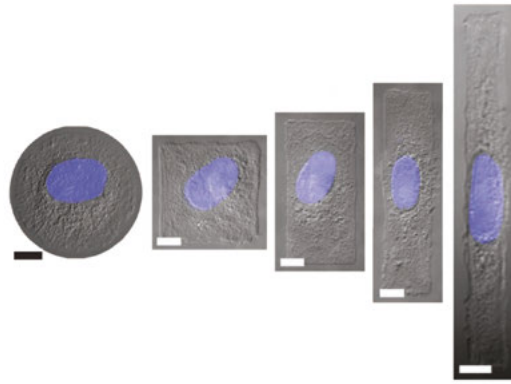
The alignment of endothelial cells due to exposure to flow has also been shown to be affected by the glucose concentration in the cell media. Human aortic endothelial cells failed to align to the flow direction under high glucose concentrations in the range between 13 mM and 30.5 mM (82). The same

behaviour was observed on primary porcine aortic endothelial cells. Here, the authors observed that the actin did not align to the flow direction after exposure to both low (2.2 mM) and high (33 mM) glucose concentrations, while the actin of cells under normal glucose conditions (5.5 mM) did align to the direction of the flow (71).

4.5 Micropatterning of Endothelial Cells

Apart from microfluidic devices, alignment of endothelial cells has also been studied on micropatterned substrates, most often consisting of line patterns of different widths. Endothelial cells tend to align more to the direction of the 2D pattern as the line width decreases and this has been observed for both primary baboon carotid endothelial cells (83) and HUVECs (84,85). Brain microvascular endothelial cells also showed this behaviour, as demonstrated on **Paper II**, where the nuclei, actin fibres and cell body of bEnd.3 cells were more aligned on 10 μm RGD patterns and their alignment decreased as the line width increased. Moreover, primary baboon carotid endothelial cells grown on 25 μm collagen patterns on glass show a similar degree of actin orientation compared to cells exposed to flow (83). Also, micropatterned endothelial cells, from the same origin, downregulated the expression of vascular cell adhesion molecule-1 (VCAM-1), a critical molecule in early plaque development. Furthermore, this behaviour is also observed when this cells were exposed to flow (86).

Furthermore, insights into cell architecture of endothelial cells have been demonstrated using micropatterning. For example, it has been shown that cell shape changes the form and orientation of the nucleus, mediated through actin fibres that exert forces on both sides of the nucleus. In this manner, increased cell elongation results in an increase in the elongation of the nucleus (**Figure 17**). This was demonstrated using a constant fibronectin micropatterned area while the geometry was varied (87).



Cell adhesive area $1,600 \mu\text{m}^2$

Figure 17. Cell Architecture. Images of single primary HUVECs, with their stained nucleus in blue, on fibronectin micropatterns of various shapes while the cell adhesive area remained constant. Scale bars= $10 \mu\text{m}$. Adapted by permission from Nature Communications. Versaevael, M., Grevesse, T. & Gabriele, S. Spatial coordination between cell and nuclear shape within micropatterned endothelial cells. Copyright 2012. Reproduced from licentiate thesis.

It has also been demonstrated that the size and shape of the micropattern affects the cell's function. For example, bovine capillary endothelial cells could adhere to $10 \mu\text{m} \times 10 \mu\text{m}$ fibronectin patterns, while cells in smaller patterns ($5 \mu\text{m} \times 5 \mu\text{m}$) underwent apoptosis (10). In **Paper I**, it was shown that bEnd.3 cells adhered to $25 \mu\text{m} \times 25 \mu\text{m}$ RGD patterns, while they did not adhere to $10 \mu\text{m} \times 10 \mu\text{m}$ patterns. However, bEnd.3 cells could adhere to $10 \mu\text{m}$ wide lines, as demonstrated on **Paper II**. Furthermore, Chen *et al.* observed that cells underwent different fates, proliferation or apoptosis, depending on the size and shape of the pattern where they can adhere and spread (10). Later, Versaevael *et al.* demonstrated that proliferation is controlled by the nuclear deformation, where more elongated nuclei showed higher levels of chromatin condensation and a decrease in DNA synthesis. Cells with less elongated nuclei, *i.e.*, rounder nuclei, exhibited lower chromatin condensation accompanied with higher DNA synthesis, indicative of a proliferative state (87).

The process of formation of new blood capillaries (angiogenesis) can also be studied using micropatterning. Angiogenesis is of interest to study vascularization *in vitro* and vascularization of materials for tissue engineering. A follow up study to Chen *et al.* demonstrated that bovine capillary endothelial cells would differentiate and undergo tube formation by changing the pattern geometry from a square to a line, by keeping the line width to $10 \mu\text{m}$ and increasing the length. Moreover, while cells on thin lines differentiated, cells on wider lines just stayed in proliferative state (88). Tube formation has been

also observed in HUVECs on PEGDA hydrogels patterned with RGD peptides using UV lithography. Tube formation was determined by the line width, where the differentiation was already observed on 50 μm wide lines, while no differentiation was observed on wider lines, up to 200 μm (89). Later, Leslie-Barbick *et al.* prepared line patterns from 10 μm up to 100 μm patterns consisting of PEG-RGDS peptides and vascular endothelial growth factor (VEGF), a signalling protein involved in angiogenesis, functionalized with PEG (PEG-VEGF) for immobilization. HUVECs formed tubes on 10 μm patterned lines with PEG-RGDS and PEG-VEGF, in a higher proportion compared to HUVECs grown on line patterns with RGDS only (84). Lei *et al.* prepared SVVYGLR peptide line micropatterns, a peptide sequence found on osteopontin that is cell adhesive, where HUVECs growing on 10 and 50 μm patterns underwent tube formation (85).

While endothelial cells from various origins have been studied on micropatterns, there is hardly any studies of brain microvascular endothelial cells on micropatterns. O'Connor *et al.* used micropatterning to study the changes in the brain microvascular endothelial cells architecture and how this affected their permeability. The patterns consisted of two fibronectin hexagons with areas of 2,500 μm^2 , resulting in cell pairs of primary human brain microvascular endothelial cells to study the cell-cell interactions. The cell pairs were treated with cyclic adenosine monophosphate (cAMP), an intracellular signalling molecule that improves barrier function in endothelial cells (90). After treatment, F-actin filaments, nuclei, and vascular endothelial cadherin (VE-cadherin) were stained for visualization and analysis. Cells treated with cAMP displayed rounder nuclei, increased VE-cadherin area at the cell-cell junction, decreased stress fibre formation and increased cortical actin compared to non-treated cells. Moreover, complementary permeability studies, showed that cAMP treated cells exhibited decreased permeability, *i.e.* increased barrier function (91). In **Paper II** it was demonstrated that the alignment of brain endothelial cells growing on 10 μm wide lines was affected by changes in glucose concentration. In this study, bEnd.3 cells were exposed to 1 mM, 25 mM and 5 mM glucose concentrations, to represent hypo- hyper- and healthy glucose levels respectively. The cells and their nuclei showed less alignment under high and low glucose conditions, while F-actin showed the opposite behaviour, where actin fibres were more aligned under high and low glucose conditions. Furthermore, the cell and nuclei were more elongated under normal glucose conditions, compared to cells under extreme glucose levels.

2D micropatterned substrates are powerful tools to understand endothelial cells behaviour under different conditions. These studies have brought to light the effect of geometry and size on cell function, such as apoptosis, proliferation, and permeability in endothelial cells (88,91,92). In recent years, due to micropatterned substrates it has been possible to observe and study cell

chirality. These studies have increased the understanding of the establishment of the left-right asymmetry in various organisms, including humans, which is of great interest in the biological and medical field. This topic was explored in **Paper III** and will be discussed in more detail in the following chapter.

Chapter 5 Cell Chirality

Left-right asymmetry or chirality is a widely conserved property in nature, observed in small molecules, such as sugars and amino acids (93). It is also seen in numerous living organisms, in vertebrates and invertebrates, including the human body (94,95). While the human body exhibit external bilateral symmetry, *i.e.*, it can be divided in two equal parts, in the interior things are not symmetrical. Internal organs adopt a left-right asymmetry or chirality, *i.e.* one side of the body is not a mirror image of the other across the midplane (96,97). For example, the left side contains most of the heart, the stomach, the pancreas, and the spleen, whereas the right side contains most of the liver and the gall bladder (**Figure 18**). Therefore, symmetry must be broken during development, however, how this process occurs is still not well understood (95).

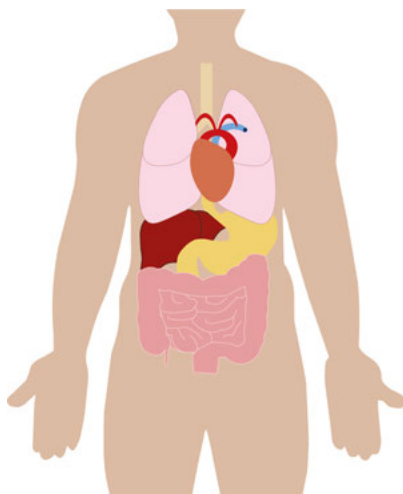


Figure 18. Left-right asymmetry at an organism level. The human interior adopts a left-right asymmetry, where one side of the body is not the mirror image of the other side across a midplane. The left side contains most of the heart, the stomach, the pancreas, and the spleen, whereas the right side contains most of the liver and the gall bladder.

The left-right axis is consistently oriented relative to the dorsal-ventral and anterior-posterior axis, determining the midline/midplane during embryogenesis (98,99). There are two proposed models describing how left-right asymmetry is established. The first model postulates that left-right asymmetry relies

on an embryonic structure known as the node, which generates fluid flow resulting in asymmetric gene expression. The second model hypothesizes that left-right asymmetry is an inherent property of the cells (95–97,100,101).

Cell chirality has been observed *in vivo*, but only in invertebrates (102). However, *in vitro* models have enabled the study of vertebrates and human cell chirality, demonstrating an inherent cell chirality under specific culture conditions (103–105). Cell chirality can be described by asymmetric alignment, migration, rotation of cells; as well as the asymmetric positioning of subcellular components and cell polarization (11,106–114). Individual cells often exhibit high randomness in morphology and migration; therefore, cell chirality is statistically defined as a population property (11,104).

5.1 Study of Cell Chirality on Micropatterned Substrates

During development cells are guided by physical boundaries imposed by the ECM, neighbouring cells, and tissues, resulting in directional alignment and migration associated with the establishment of left-right asymmetry. By using micropatterns it is possible to culture cells on well-defined appositional boundaries to mimic the physical boundaries during development, and therefore study the mechanisms dictating left-right asymmetry (104,115). Commonly used micropattern geometries are lines and rings, that provide two appositional boundaries (Figure 19). Generally, these micropatterns are between 100 to 200 μm in width. The appositional boundaries offer a primary direction for the cells to elongate and orient. Then the cells have to make a decision on which direction to orient and/or migrate, which is amplified by the opposing boundaries leading to a chirality bias (11).

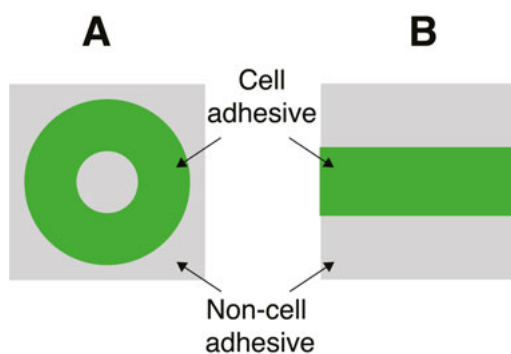


Figure 19. Micropattern geometries for cell chirality studies. A. Ring. B. Line. Cell adhesive region depicted in green. Non-adhesive region, depicted in grey.

In micropatterned substrates the cell alignment is calculated using image analysis software (discussed further in Chapter 6). On a ring micropattern, the cell

alignment is based on its deviation from the circumferential direction, where a positive value (0° to 90°) is designated counter-clockwise (CCW) alignment, while a negative value (-90° to 0°) represents a clockwise (CW) alignment (11), as schematically presented in **Figure 20A**. Line micropatterns have also been used for the analysis of cell chirality where cell chirality is often reported as positive or negative. In **Paper III**, CellProfilerTM, an open source image analysis software to obtain the cell orientation was used (116). CellProfilerTM calculates the orientation of the cell by fitting the segmented cell to an ellipse. The orientation then corresponds to the angle between the x-axis (determined by the RGD pattern direction) and the major axis of the ellipse, giving values within $\pm 90^\circ$ (116,117) (**Figure 20B**). In this manner, the cell angle orientation gets negative (-90° to 0°) values or positive values (0° to 90°), respectively, relative to the line pattern (**Figure 20B**).

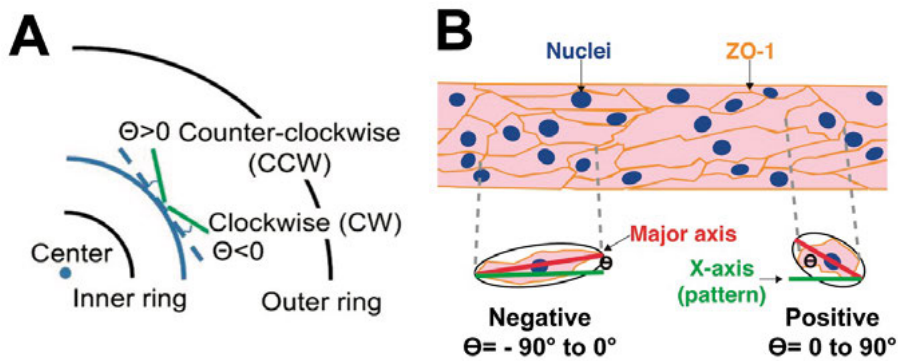


Figure 20. Cell chirality micropatterns. A. Cell alignment on ring micropatterns. Cell alignment bias in ring micropatterns is determined by the deviation of cell alignment from the circumferential direction, where a cell gets at angle between -90° to 0° and is defined as clockwise (CW) alignment, while a cell with an angle between 0° to 90° value represents a counter-clockwise (CCW) alignment. Adapted with permission from B. The cell chirality in line micropatterns is determined by the cell angle orientation relative to the line pattern, which gets negative (-90° to 0°) values or positive values (0° to 90°). A is adapted with permission from Wan, L. Q., Ronaldson, K., Park, M., Taylor, G., Zhan, J. M. & Vunjak-Novakovic, G. Micropatterned mammalian cells exhibit phenotype-specific left-right asymmetry. *Proc Natl Acad Sci U S A*. 2011;108(30):12295–300.

Cell chirality can also be defined by the cell's organelle positioning, resulting from the relationship between the apicobasal axis and the front-rear axis. The apicobasal axis is defined as a result from 2D cell attachment, while the front-rear axis is defined by the nucleus-centrosome axis *i.e.*, the x axis is defined as the direction from the nucleus to the centrosome as schematically presented in **Figure 21A** (11,103,104,118). It has been shown that cells growing on micropattern (lines and rings) are polarized at the boundaries, defining the front-rear axis of the cells, where the cells position their centrosomes and Golgi

apparatus towards the boundary(**Figure 21B**) (11,114). It has been shown that the cell chirality bias based on micropatterned substrates is consistent with the chirality of organelle positioning (119). Using the definition of cell polarization, counter clockwise alignment on rings can be considered as a cellular ‘leftward’ bias, and clockwise as a ‘rightward’ bias (11,103,118)

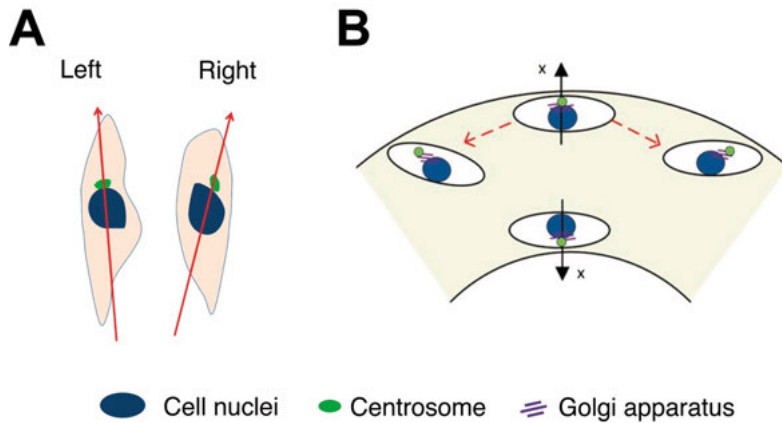


Figure 21. Organelle positioning. The apicobasal axis is defined as a result from 2D cell attachment, while the front-rear axis is defined by the nucleus-centrosome axis. **A.** A red arrow is drawn from the centre of the nucleus, depicted in blue, to the centrosome, depicted in green. Cells migrating or orienting to the left of the nucleus-centrosome axis are defined as leftward bias, while cells migrating or orienting to the right are defined as rightward bias (11,103,118). **B.** Cell polarization on micropatterns. Cells polarized at the boundary by positioning their centrosomes (green) and Golgi apparatus (purple) closer to the boundary than nuclei (blue). A is adapted by permission from Springer Nature, Stem Cell Research & Therapy, Micropatterning of cells reveals chiral morphogenesis. Wan, L.Q., Ronaldson, K., Guirguis, M., Vunjak-Novakovic, G., 2013. B is adapted with permission from Wan, L. Q., Ronaldson, K., Park, M., Taylor, G., Zhan, J. M. & Vunjak-Novakovic, G. Micropatterned mammalian cells exhibit phenotype-specific left-right asymmetry. *Proc Natl Acad Sci U S A.* 2011;108(30):12295–300.

It has now been widely observed that cell chirality varies depending on cell type (**Table 1**). For example the bias of endothelial cells is different to muscle cells, exhibiting clockwise and counter-clockwise bias respectively (11). Endothelial cells exhibit clockwise bias, regardless of the blood vessel they line, where human umbilical vein and human brain microvascular endothelial cells both exhibited a clockwise bias (111,120). In **Paper III** we demonstrated that mouse brain microvascular endothelial cells also exhibited a negative bias, where the cell chirality bias was most pronounced on 100 μm wide lines.

Table 1. Cell chirality varies depending on cell type. Positive angles stand for counter clockwise (CCW) bias, while negative alignment angles stand for clockwise bias in ring micropatterns.

Cell type	Bias	Species	Tissue	Phenotype	Cell origin	Pattern type	Ref.
Human umbilical vein endothelial cells (HUVEC)	CW	Human	Umbilical vein	Endothelial cells	Primary	Ring	(11,111,121)
Human brain microvascular endothelial cells	CW	Human	Brain capillary	Endothelial cells	Primary	Ring	(120)
bEnd.3	Negative	Mouse	Brain capillary	Endothelial cells	Cell line	Line	Paper III
Human skeletal muscle cells (hSkMC)	CCW	Human	Skeletal muscle	Myoblast	Cell line	Ring	(11)
C2C12	CCW	Mouse	Skeletal muscle	Myoblast	Cell line	Ring	(11)
C2C12	Negative	Mouse	Skeletal muscle	Myoblast	Cell line	Line	(109,110)
Rat cardiac fibroblast	CW	Rat	Heart	Cardiac fibroblast	Primary	Ring	(11)
Human adipose stem cells (hASC)	CW	Human	Adipose	Stem cells	Primary	Ring	(11)
Human mesenchymal cells (hMSC)	CW	Human	Bone marrow	Stem cells	Primary	Ring	(11)
Human primary skin fibroblast	CW	Human	Skin	Fibroblast	Primary	Ring	(11)
Human skin fibroblast line	CW	Human	Skin	Fibroblast	Cell line	Ring	(11)
Human skin cancer fibroblast line	CCW	Human	Skin	Fibroblast	Cell line	Ring	(11)
NIH/3T3	CW	Mouse	Embryo	Fibroblast	Cell line	Ring	(11)
MDCK	CCW	Dog	Kidney	Epithelial	Cell line	Ring	(108)
MDCK	Positive	Dog	Kidney	Epithelial	Cell line	Line	(114)
MC3T3-E1	CW	Mouse	Calvaria	Osteoblast	Cell line	Ring	(11)

Recent studies have also demonstrated that protein kinase C (PKC) activation or treatment with carbon nanotubes induces cell chirality reversal, suggesting that cell chirality might be affected in disease states (111,120–122). Endothelial cells experienced cell chirality reversal due to PKC activation induced by indolactam V (111,120). PKC is a mediator of vascular permeability which has also been implicated in disorders associated with hyperglycaemia in diabetes mellitus (106,111,120,122,123).

Major discoveries in cell structure and function have been achieved using micropatterned substrates as demonstrated in this section and Chapter 4. However, these studies would not have been possible to assess without immunofluorescence, high resolution imaging and image analysis. These methods are non-trivial and will be discussed in more detail in Chapter 6.

Chapter 6 Analysis of Cell Morphology and Function *In Vitro*

An important technique in the analysis of biological samples is the selective incorporation of fluorescent molecules to different cell components and their detection using fluorescent microscopy. Immunofluorescence is a widely used technique which combines the selective binding of antibodies to specific molecules in fixed cells and their conjugation to fluorescent labels. In this manner, various cell components can be identified and located using fluorescent microscopy. In recent years, new methods have been developed so-called live stains, that permit the fluorescent labelling of various cell components on living cells and follow their changes in real time. Moreover, various image analysis methods and software have been developed to quantify phenotypical features from the acquired microscopy images of cells.

6.1 Immunofluorescence

Immunofluorescence is a technique based on an antibody binding to the protein of interest in a cell sample, followed by visualization of the bound antibody by conjugating the antibody to a fluorophore. Immunofluorescence requires fluorescent microscopy (discussed in Section 5.4) and allows to capture images to determine the cellular localization of the protein of interest (124). Immunofluorescence can be used in various sample types, such as tissue samples, entire organisms and on cultured cells (124,125). Immunofluorescence protocols have been adapted to cultured cells under different culture conditions, such as inside microfluidic devices, as demonstrated in Paper IV, or for cells growing on hydrogel samples, as demonstrated in Paper II and III (21).

Immunofluorescence exploits the fact that antibodies can selectively react to unique protein molecules. Briefly, antibodies are proteins produced by cells of the immune system. Antibodies can react against molecules that the host organism recognizes as foreign substance, also known as antigens, such as pathogenic bacteria and viruses, and generate an immune response. Moreover, the immune system can produce various antibodies which each will specifically recognize a unique antigen, for example a protein coat of a virus (124). Antibodies can be produced by immunizing an animal, *i.e.*, introduce a foreign

protein and let them produce antibodies, and then retrieve them from their serum. In this manner antibodies against various human proteins have been produced. However, in recent years there has been development of non-animal methods to produce antibodies.

Antibodies are proteins that consist of two identical polypeptide heavy chains and two identical light chains forming a Y shape (**Figure 22**). Two different antigen binding fragments are identified in the antibody structure, the antigen binding fragment (Fab) and the crystallizable fragment (Fc). Moreover, the Fab domains contain the variable fragment (Fv), which have different amino acid sequences in different antibodies, and it is this diversity that enables different antibodies recognize specific antigens. While the Fc fragment is conserved within species (124).

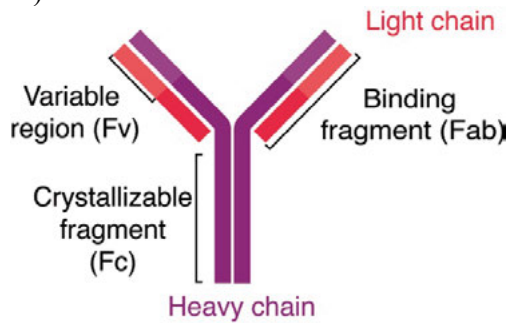


Figure 22. Antibody Structure. Antibodies consist of two identical polypeptide heavy chains and two identical light chains forming a Y shape. They contain two antigen binding fragments, the antigen binding fragment (Fab) and the crystallizable fragment (Fc). The Fab domain contains a variable fragment (Fv), which varies among antibodies to recognize specific small regions in the antigens known as epitopes. Reproduced from licentiate thesis.

There are two immunofluorescence methods, direct or indirect immunofluorescence. Direct Immunofluorescence utilizes a fluorophore conjugated primary antibody that will be reacting with the target antigen in the sample. While indirect Immunofluorescence, utilizes first an unconjugated primary antibody which binds to the antigen. Then a secondary antibody, fluorescently labelled, recognizes and binds to the primary antibody (**Figure 23**). The secondary antibody must originate from the same species of the primary antibody, in this manner the secondary antibody will bind to the Fc fragment and can detect all primary antibodies generated in that species. For example, if a ZO-1 primary antibody was raised in rabbit, the secondary must react with rabbit antibodies, *i.e.*, anti-rabbit. Direct methods are shorter and allow the detection of multiple antigens. However, it shows lower sensitivity, where signal is often higher in indirect methods due to multiple fluorescently labelled secondary antibodies that can bind to one primary antibody (124,125).

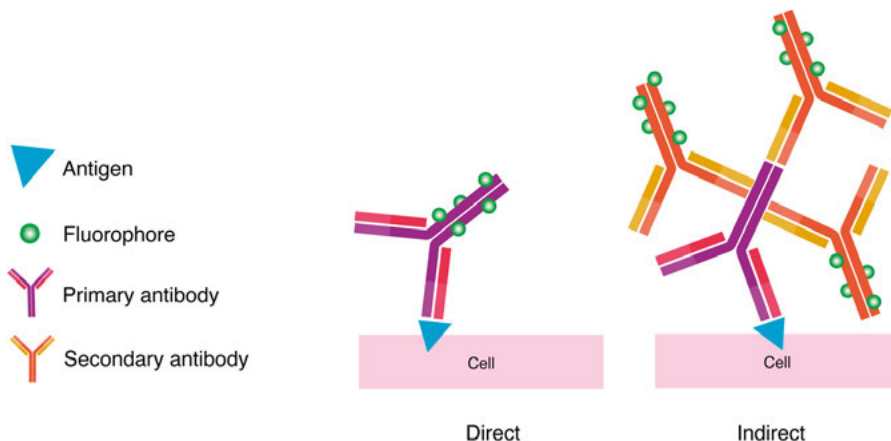


Figure 23. Direct and indirect immunofluorescence. Direct immunofluorescence relies on a primary antibody conjugated to a fluorophore. The primary antibody will directly bind to the desired antigen and can be visualized thereafter. Indirect immunofluorescence utilizes two antibodies, a primary antibody, and a secondary antibody. The primary antibody binds to the antigen and secondary antibody, fluorescently labelled, will bind to the primary antibody. Generally, indirect immunofluorescence has higher sensitivity, since more than one fluorescently labelled secondary antibody can bind to the primary antibody, resulting in higher fluorescent signals. Reproduced from licentiate thesis.

Independently of the immunofluorescence method, direct or indirect, the following steps are often followed: fixation, membrane permeabilization (if the target epitope is buried within the membrane), blocking, primary antibody incubation, with or without secondary antibody incubation. There is no universal immunofluorescence protocol, and it will vary depending on the antibody, epitope and type of sample, and it requires testing and optimization.

The first step is the fixation of the cells with the purpose to halt cellular activity and preserve the cells, to retain the cellular distribution and preserve cellular morphology. Solvents, such as methanol and acetone can be used, which work by extracting lipids and precipitating proteins. Moreover, they are also effective as simultaneous permeabilization agents. Paraformaldehydes work by crosslinking free amino groups, and it is commonly used for the staining of membrane associated proteins (126). However, for the staining of hydrogel-based samples, paraformaldehyde is preferred, due to possible swelling or collapsing of the hydrogel when using solvents, resulting in deformation of the sample.

After fixation, the sample might still require membrane permeabilization to facilitate antibody penetration in the cell. This step is performed using different detergents such as saponin, Triton-X 100 or Tween 20. Different detergents and concentrations may give different results, and the optimal

parameters should be determined experimentally, where minimal cellular morphology distortion with optimal antibody penetration is achieved (124).

During primary and secondary antibody incubation, non-specific interactions between the antibodies and the biological sample might occur, due to low affinity of the antibody to the antigen or the trapping of the antibody in hydrophobic structures (124). This can be attenuated by a blocking step, using a blocking buffer solution containing proteins is added to the sample. The proteins essentially can bind to all proteins present in the sample and the antibodies will compete with the blocking protein to bind their antigen. Common blocking buffers contain bovine serum albumin (BSA) or serum (125). The blocking buffer should be obtained from a different species than the primary antibody origin. Moreover, if indirect immunofluorescence is performed, the blocking serum should have the same origin species as the secondary antibody (124). For example, a ZO-1 primary antibody was raised in rabbit, and the secondary anti-rabbit was raised in goat, the optimal blocking buffer would contain goat serum.

After the previous steps, the sample is ready for antibody incubation. The primary antibody is diluted in the blocking buffer and added to the sample. After incubation, the unbound antibody is removed by multiple washes with PBS containing a detergent (Triton-X 100 or Tween 20) in low concentrations. In the same manner, the secondary antibody is added and removed if indirect immunofluorescence is performed.

Often by the end of the immunofluorescence other cellular components are commonly stained, such as the nuclei and the cytoskeleton and they do not require the use of antibodies. For example, the nucleus is often stained using 4',6-diamidino-2-phenylindole (DAPI) or Hoechst 33342. Both DAPI and Hoechst 3342 interact with DNA and emit fluorescence in the blue spectrum. The staining of actin filaments in the cytoskeleton is usually achieved using phalloidin conjugated to a fluorescent dye. Phalloidin is a bicyclic peptide that binds selectively to the actin filament. While DAPI and phalloidin are cell permeable, they are toxic to the cells and therefore are not used in living samples. However, in recent years there has been great advance in the development of live stains, *i.e.*, stains that work on living cells in culture and will be discussed in the following section.

6.2 Live Imaging

One of the first and widely used stains in living samples is the so-called Live/Dead® staining. It consists of two fluorescent dyes, calcein-am and propidium iodide, that interact with live or dead cells respectively. Calcein-am is

permeable to cells and becomes green-fluorescent after hydrolysis by intracellular esterase enzymes, ubiquitous in live cells. On the other hand, propidium iodide is non-cell permeable and can only enter damaged membranes, an indicator of dead cells. The dye will fluoresce upon binding to DNA, resulting in predominant red fluorescence in the nuclei area. This stain is widely used to assess cytotoxicity and cell viability. However, the cell sample cannot be further used.

There are now various types of available products to stain cellular components to observe morphological and migration changes in the cell culture. It is possible to stain the nuclei, actin filaments, tubulins, lysosomes, and the whole cell (*e.g.*, CellTracker™) on living samples. These dyes have opened the possibilities to track changes in the cell components in real time. Another advantage of live staining is that it does not require fixation and all the time-consuming steps of immunofluorescence protocols, and the samples can be kept alive and still studied, instead of end-point samples. However, the availability of live stains is limited to common cell components (nuclei, actin, etc.) while dyes for more specific proteins to different cell types are not available, and immunofluorescence must be used instead.

A very important aspect of using live staining is that during imaging the cells must be maintained in cell culture conditions (*i.e.*, 37°C, humidity, and pH-controlled environment) otherwise it will cause cell decay and death. These conditions can be maintained using a so-called microscope incubator, which consist of a chamber on top of the microscope stage that can control temperature and CO₂. However, they are bulky and often expensive (**Figure 24A**). Stage incubators are a smaller and cheaper alternative to microscope incubators. They consist of a transparent chamber the size of traditional cell culture plate with temperature control, CO₂ and O₂ supply (**Figure 24B**). However, the use of such set ups, and microscope incubators, reduces the access of the microscope for other users, where often the sample cannot be moved until the experiment is finished, even if image acquisition is not running, as this might cause perturbations in the cell culture conditions, affecting the experimental outcome. One possible solution is to construct a customized device to fit one's specific needs, as shown in **Paper IV**. In this approach a microfluidic carrier was developed (**Figure 24C**). The carrier, which has the outer dimension of a standard culture well plate, accommodates a microfluidic device, an integrated perfusion system for the microfluidic device, and a temperature feedback control to maintain the microfluidic chip temperature at 37 °C when outside the incubator. This carrier is an affordable, user-friendly system that maintains physiological conditions during imaging and minimizes the microfluidic device manipulation during transport from the microscope and incubator in between imaging sessions.

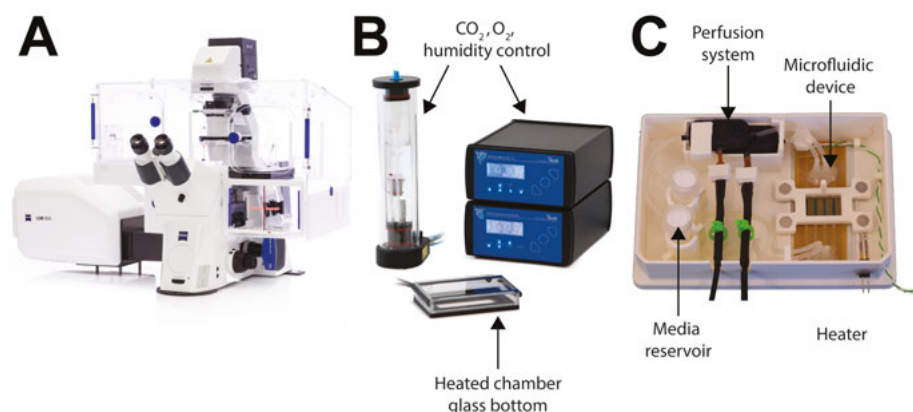


Figure 24. Set ups for live imaging microscopy. **A.** Microscope incubator. It consists of a chamber surrounding the microscope and offers controlled warm air incubation. Photo: Zeiss **B.** Stage top incubators consist of a small chamber that is placed on the microscope stage. They are equipped with CO₂, O₂ and humidity control and fit a standard culture plate. Courtesy of ibidi GmbH. **C.** Customized microfluidic carrier. Carrier design to be used during microscopy and transport of a microfluidic device. The carrier is the size of a standard culture plate and contains heat and media perfusion control. This carrier minimizes the microfluidic device manipulation and maintains physiological conditions during microscopy. Reproduced with permission from **Paper IV**.

6.3 Fluorescent Microscopy

Fluorescent microscopy is required for visualization of fixed and fluorescently labelled living samples. Fluorescence is a type of luminescence due to the absorption of light of a molecule and ending with the emission of light. The wavelength of the emitted fluorescent is generally longer than the wavelength of the absorbed light. For example, a very common fluorescent dye used is fluorescein, or FITC, which has an excitation wavelength of 490 nm and an emission wavelength of 525 nm.

A fluorescent microscope can accommodate several laser lines with a wide range of wavelengths (from UV to the infrared) to excite various fluorophores with different excitation wavelengths. However, conventional wide field fluorescent microscopes often give blurry images with low contrast. This is due to the entire depth of the sample is being illuminated and fluorescent signals are collected from all regions, *i.e.*, from the focus plane and the areas below and above it. Confocal microscopy is often desired for high resolution imaging, due to their ability of eliminating out of focus light, by selectively collecting light from a thin (<1 μm) section of the sample. Moreover, they can capture multipanar images which can be integrated to produce a 3D representation of the sample (124,125,127).

A confocal microscope works similar to a wide field fluorescent microscope; however, a confocal microscope is equipped with a pinhole, which blocks the light from the out of focus areas. Briefly, during imaging in a confocal microscope, the objective focuses light from a laser to a limited spot (focal spot) in the sample. The fluorescent probes are excited and emit fluorescent light in all directions. The irradiation is most intense at the focal spot, but the areas above and below the focal spot in the sample are also illuminated. The output light from the laser is reflected by a beam splitter. A scanner deflects the laser beam into the objective, so the laser scans across the sample. Then, the fluorescence emissions from the fluorophores in the sample are collected by the objective and follows the reverse path back to the beam splitter and to a detector. When multiple fluorophores are used, the splitter transmit the emissions to separate detectors. The fluorescence captured is then focused by the pinhole. The pinhole diameter can be adjusted to block more or less the out-of-focus light, affecting the axial resolution. Values between 0.7 to 1.0 airy unit allows most of the in-focus light to reach the detector and blocks most of the out-of-focus light (127).

When multiple cell components are being stained it is of special importance to carefully choose the fluorophores. The choice of fluorophores is first based on the available laser lines in the microscope. Second, different fluorophores are selected for each of the targets. The optimal choice is to select fluorophores that are excited by different lasers as well as different excitation spectra to minimize spectral overlap.

6.4 Image Analysis

Each microscopy image contains a huge amount of information. It was not until the popularization of image analysis in the biological field, that this information was made available. The development of image analysis techniques has permitted various biological discoveries and nowadays quantitative image analysis is a vital tool in many labs (128). One of the main applications of biological image analysis is cell phenotype quantification and structure visualization. In order to obtain quantitative information from specific images, custom tools have been developed using programming software, such as python and MATLAB. However, some tools have been developed for general use and have been widely adopted by researchers, such as ImageJ (129) and CellProfiler™, which is particularly useful for high throughput cell image analysis (116).

The most basic pipeline of image analysis of biological samples is the following: image acquisition; pre-processing; segmentation; and feature extraction. During image acquisition a digital image is acquired, which was covered in

the previous section. The rest of the steps can be performed using cell image analysis software such as ImageJ and CellProfiler™ and will now be briefly described.

After image acquisition, images often go through a pre-processing step. This step aims to enhance the image for better visual inspection by reducing noise in the image. This is achieved by the application of different types of filters, such as smoothing filters and edge enhancing filters. The choice of filter will depend on the type of cell component and the type of noise in the image. For example, edge enhancing filters are often used to enhance the actin filament in the images. These steps do not increase the image information but helps in the successful identification of objects in the following steps.

The most basic image processing step is segmentation, where the object of interest is distinguished from the background. This step is very important since accurate segmentation of the objects of interest in an image is crucial for studying the object properties, such as counting the number of objects and measure their geometric properties (*e.g.*, orientation, perimeter, area). Segmentation is difficult and there is no universal method. Generally, segmentation methods are based on two basic properties of the intensity values in the image, similarity and discontinuity. Similarity, or region-based methods, rely in partitioning the image into regions that are similar based on a set criterion. Discontinuity, or edge-based methods, detect the edge regions where the intensity values go from light to dark. Thresholding, a region-based method, is one of the most common approaches used in segmentation. Briefly, an initial grey level intensity or threshold value T is set. All pixels in the image will be classified based on the T value. If the pixel intensity value is greater than T the pixel is part of an object or else the pixel belongs to the background. Watershed segmentation, an edge-based method, identifies edges (regions where pixels go from dark to light) and the regions inside the edges are objects (130).

After the objects have been identified in the segmentation process information can be extracted. For example, with CellProfiler™, a large number of features of each segmented object can be calculated, such as orientation and eccentricity (116). CellProfiler™ calculates the orientation of an object by using an ellipse-fitting model (116,117,131). Where the fitted ellipse has same second-moments as the object, *i.e.*, the ellipse has the same perimeter and area as the segmented object, as schematically represented in **Figure 25A**. The orientation then corresponds to the angle between the x-axis and the major axis of the ellipse resulting in orientation values of $\pm 90^\circ$ (116,117). A horizontally aligned object to the x-axis has a 0° angle, while an object whose major axis points to the upper right has a negative orientation (-90° to 0°). On the other hand, an object that points to the left will have a positive orientation (0° to 90°) (**Figure 25B**). The eccentricity is the ratio of the distance between the

foci of the ellipse and its major axis length (**Figure 25C**). A value of 0 corresponds to a circle, while an ellipse whose eccentricity is 1 is a line segment (116,117).

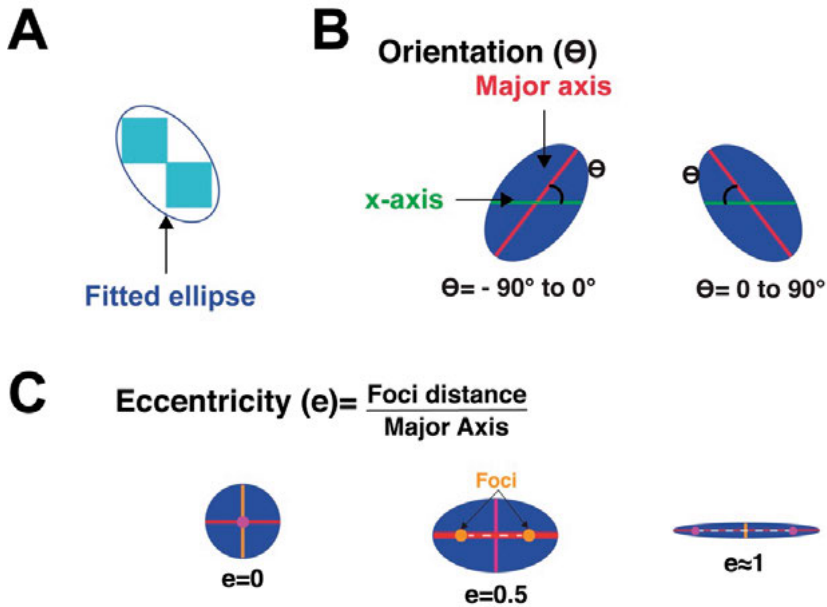


Figure 25. Orientation and eccentricity calculation. **A.** The segmented object (depicted in light blue) is fitted into an ellipse. **B.** The orientation is the angle between the x axis (depicted in green) and the major axis (depicted in red). **C.** The orange dots correspond to the ellipse foci. The eccentricity is the ratio of the distance between the foci of the ellipse and its major axis length. A value of 0 corresponds to a circle, while an ellipse whose eccentricity is 1 is a line segment.

Immunofluorescence and image analysis are powerful tools used in biological research for the evaluation of cell phenotypes. Immunofluorescence enables the visualization of subcellular components and their distribution in the cell. Then, the images acquired can be processed by image analysis to obtain quantitative description of the components of interest. This process takes a step after step manner; however, all steps depend on each other, resulting in a rather iterative process. For example, the image resolution selected during image acquisition will have an effect in the quality of the object detection. Small features such as actin fibres will not be able to be segmented properly if the image resolution is very low, while the nucleus, is easier to segment due to its elliptical shape. Furthermore, high throughput image analysis tools permit the analysis of large image data sets from various cell components. This allows to detect phenotypes and trends that otherwise would be missed by simple human visual inspection.

Chapter 7 Conclusions and Outlook

This thesis demonstrates the fabrication of cell culture substrates for the study of brain microvascular endothelial cell function. First, a photocrosslinkable HA hydrogels (HA-am) was synthesized to prepare covalently photocross-linked HA hydrogels via micromoulding (**Paper I**). Second, photolithography was used to control, with high precision, the presence of cell adhesive molecules and its geometrical distribution. In this manner, it was possible to control the cell adhesion of brain endothelial cells on the micrometre scale (**Papers I, II and III**) and study their changes in morphology. 2D micropatterned substrates are powerful tools to understand endothelial cells' structure and function. However, these studies would not have been possible to assess without immunofluorescence, confocal microscopy, and image analysis. To perform this, an immunofluorescence protocol for the staining of nuclei, F-actin and ZO-1 of bEnd.3 cells on micropatterned substrates and microfluidic chips was developed (**Papers II and IV**). Furthermore, the high-throughput image analysis was used for the extraction of quantitative properties of the cells in these images (**Papers II and III**).

Micropatterned *in vitro* substrates allows the study of the effects and mechanisms of cell function in a controlled manner. While a lot of research has been done using micropatterned substrates and hydrogel substrates to better mimic the *in vivo* situation, there is a necessity in standardization to better compare studies across laboratories and cell types. For example, cell chirality analysis, an inherent cell property was demonstrated using micropatterned substrates. This property presents an easy comparative measurement among cell types, due to its binary nature. However, different pattern sizes and cell orientation analysis are used. As a first step to reach standardization the effect of pattern size was assessed in **Paper III**. Furthermore, CellProfilerTM, an open source and widely use image analysis software, was used for the cell orientation and cell chirality determination of brain endothelial cells.

The endothelial cell microenvironment *in vivo* is extremely complex and is always changing, for example caused by diseases or toxic substances entering the blood stream. In this thesis, changes in the structural cues given by the ECM were modelled by changing the cell adhesive areas in the hydrogel (**Papers II and III**). Then, the effects of glucose levels on brain endothelial cells

morphology in these limited areas were assessed (**Paper II**). However, *in vivo*, the endothelial cell microenvironment can also vary in other ways. For example, the ECM can change in composition or mechanical properties, due to disease. Through microfabrication methods it is possible to develop standardized and high-throughput *in vitro* models that permit the variation of various parameters, at the same time, such as the ECM composition and mechanical properties to study their effect at the cellular level.

While great advances to better mimic the cell microenvironment have been done, there is still work to do to incorporate the dynamic nature of the cell microenvironment *in vitro*; and ultimately contribute to the understanding of the effect of the cell microenvironment on endothelial cell function.

Chapter 8 Summary of Included Papers

8.1 Summary of Paper I

In Paper I, two microfabrication techniques, micromoulding and photolithography were used to prepare photocrosslinkable hydrogels for cell culturing of brain endothelial cells. First, HA derivative (HA-am) was synthesized to present acrylamide groups on their backbone. The acrylamide groups can cross-link with each other in the presence of a photoinitiator and subsequent UV exposure. In this manner, HA-am hydrogels were fabricated using a Si-SU8 mould to control its shape and dimensions. Furthermore, by varying the UV exposure times the hydrogel stiffnesses were varied, where the stiffness increased with longer exposure times. Then, the otherwise non-cell adhesive HA-am hydrogel was functionalized with cell adhesive RGD peptides. This step was achieved using photolithography, where the unreacted acrylamide groups after hydrogel crosslinking could be used in the photopatterning of RGD peptides. RGD peptides were designed to contain thiol groups by presenting a cysteine amino acid (GCGYRGDSPG), which can react with the acrylamide groups in the presence of a photoinitiator and UV light, via thiol-ene reactions. By varying the UV exposure, RGD peptides would bind to the exposed areas in the photomask to various extents, while keeping the RGD peptide concentration constant. It was observed that shorter exposure resulted in less RGD binding to the hydrogel and did not provide enough adhesive molecules for the cells to attach. On the other hand, longer UV exposure caused overexposure, resulting in RGD binding and cell adhesion outside the exposed areas. The pattern size also affected cell adhesion, while the smallest pattern size achieved was $5\text{ }\mu\text{m} \times 5\text{ }\mu\text{m}$, cells did not adhere to these patterns. The minimum pattern size to which cells adhered was $25\text{ }\mu\text{m} \times 25\text{ }\mu\text{m}$ (**Figure 26A**), while more cells adhered to $100\text{ }\mu\text{m} \times 100\text{ }\mu\text{m}$ patterns (**Figure 26B**).

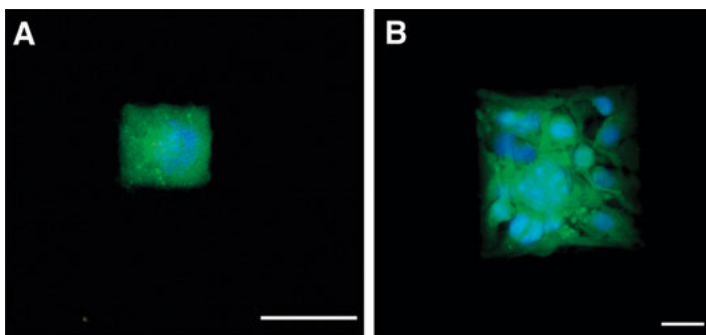


Figure 26. Fluorescent images showing bEnd.3 cells growing selectively on square peptide GCGYRGDSPG patterns on the hydrogel surface on day 1 A. bEnd.3 cells on 25 µm x 25 µm RGD peptide patterns B. bEnd.3 cells on 25 µm x 25 µm RGD peptide patterns. Scale bars= 25 µm. Live cells within the pattern are stained in green and dead cells (non- observed) are stained in red. The cell nuclei are stained in blue. Adapted from Porras Hernandez, A. M., Pohlitz, H., Sjögren, F., Shi, L., Ossipov, D., Antfolk, M., Tenje, M. (2020) A simplified approach to control cell adherence on biologically derived in vitro cell culture scaffolds by direct UV-mediated RGD linkage. *Journal of Materials Science: Materials in Medicine* 31:89. Reproduced from licentiate thesis.

8.2 Summary of Paper II

In Paper II we utilized the developed platform from Paper I to investigate if brain microvascular endothelial cells could align to RGD patterns. For this purpose, we prepared RGD micropatterns on HA-am hydrogels with varying line widths (10 - 100 µm). Mouse brain microvascular endothelial cells (bEnd.3) were seeded on the micropatterns for 24 h, then fixed, stained their nuclei, F-actin and ZO-1; and imaged using confocal microscopy (**Figure 27**). The acquired images were processed and analysed using CellProfiler™, a high throughput image analysis software. From the image analysis, quantitative measurements of the orientation of the nuclei, actin fibres and cell bodies; and the elongation of the nuclei and the cells were obtained. The data showed that brain microvascular endothelial cells nuclei, actin fibres and cell bodies orient to the direction of the pattern, and even more so as the line width decreases. Nuclei and cell elongation increased as the line width decreased. Cells on non-patterned substrates show a widely distributed nuclei, actin and cell orientation. Moreover, the bEnd.3 cells showed decreased nuclei or cell elongation on non-patterned substrates, compared to cells growing on line patterns.

In this paper we also investigated the emulated hypo and hyperglycaemia states to assess the effect on brain microvascular endothelial cells on micropatterned substrates. For this purpose, bEnd.3 cells growing on 10 µm micropatterns were exposed to 1 mM, 25 mM and 5 mM glucose concentrations,

often used to represent hypo- hyper- and healthy glucose levels respectively. The cells and their nuclei showed less alignment under high and low glucose conditions, while F-actin showed the opposite behaviour, where actin fibres were more aligned under high and low glucose conditions. The cell and nuclei were more elongated under normal glucose conditions, compared to cells under extreme glucose levels.

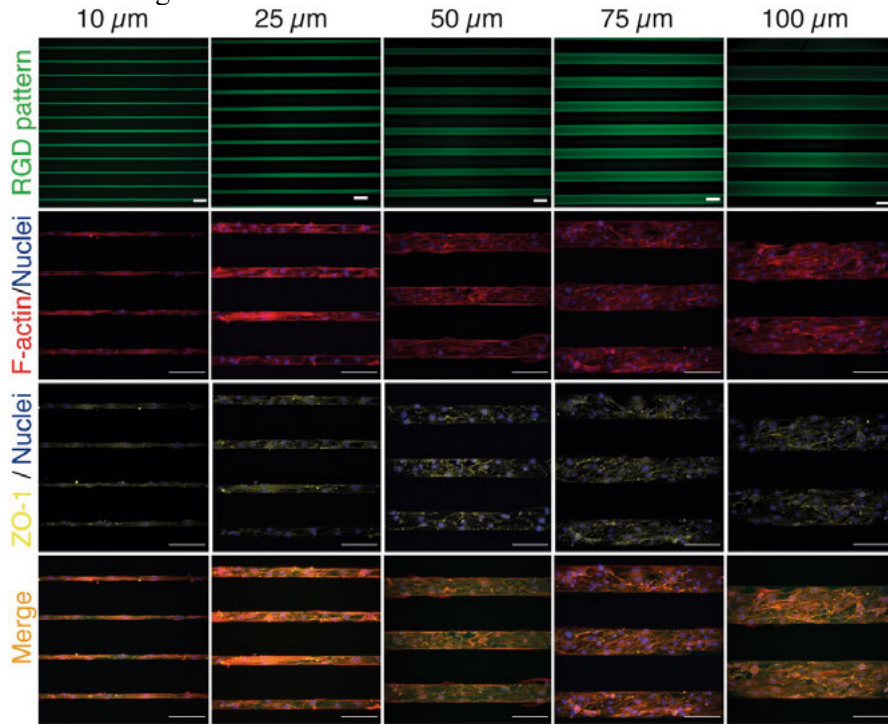


Figure 27. Micropatterned bEnd.3 cells on line patterns with varying widths. Brain microvascular endothelial cells (bEnd.3) adhere to RGD pattern lines. First row: Lines of fluorescent 5-FAM-GCGYRGDSPG peptide patterned on HA-am hydrogels (green). Second row: bEnd.3 cells seeded on the lines stained for F-actin (red) and nucleus (blue). Third row: bEnd.3 cells seeded on the lines stained for zonula occludens-1 (ZO-1) (yellow) and nucleus (blue). Forth row: Merged images showing the cells on the micropatterned lines illustrating that the cells are adhering only to the peptide-patterned lines. Scale bars= to 100 μm . Adapted from Porras Hernández, A. M., Barbe, L., Pohlitz, H., Tenje, M., Antfolk, M (2021) Brain microvasculature endothelial cell orientation on micropatterned hydrogels is affected by glucose variation. *Scientific Reports* 11:19608. Reproduced from licentiate thesis.

8.3 Summary of Paper III

In Paper III we investigated if brain microvascular endothelial cells exhibited a cell chirality bias on line micropatterns (**Figure 28A**) and to determine the optimal line width to study the effect on cell chirality under disease states or treatment with toxic substances. Cell chirality was determined by the cell alignment bias to the underlying micropatterned (**Figure 28B**). Overall, brain microvascular endothelial cells exhibited a negative chirality bias on line micropatterns ranging from 10 μm to up to 400 μm , compared to non-patterned substrates, where cell chirality bias is not exhibited (**Figure 28C**).

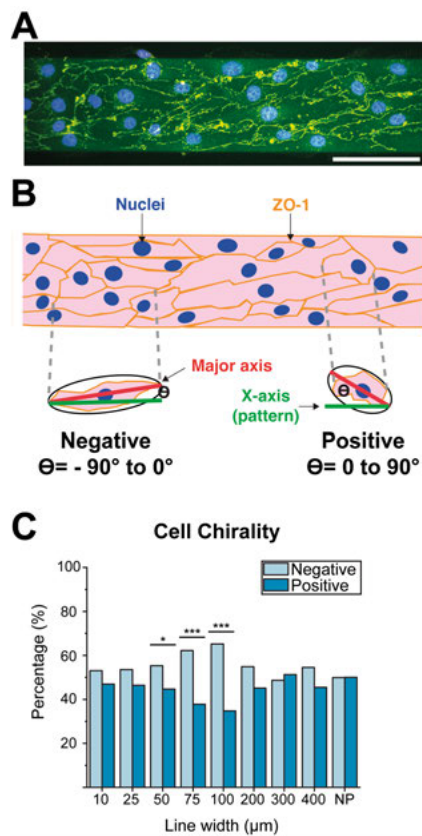


Figure 28. Cell chirality of micropatterned brain microvascular endothelial cells.
A. Stained brain microvascular endothelial cells, nuclei in blue, ZO-1 in yellow and RGD pattern in green. **B.** Schematic of cell orientation calculation. **C.** Bar plot of the percentage of cells exhibiting a negative or positive bias depending on the line width.

8.4 Summary of Paper IV

In Paper IV a customized microfluidic carrier was developed for the study of brain microvascular endothelial cells under various flow regimens. The purpose of the carrier was to minimize the disturbance of the cell culture, by minimizing the microfluidic device manipulation, flow and temperature disturbances during transport from the microscope and incubator in between imaging sessions. The carrier had an outer dimension of a standard culture well plate and accommodates microfluidic device, an integrated perfusion system for the microfluidic device, and a temperature feedback control (**Figure 29A**). Furthermore, the live imaging of nuclei and F-actin, and the immunofluorescence staining of ZO-1 proteins of brain microvascular endothelial cells was achieved inside the microfluidic chip (**Figure 29B and C** respectively).

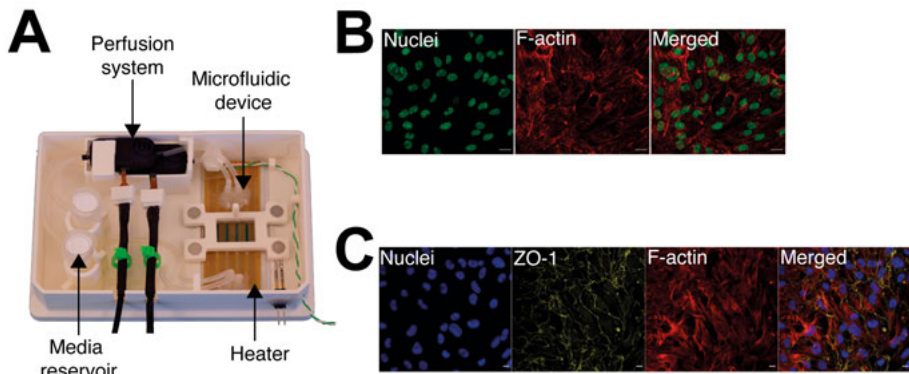
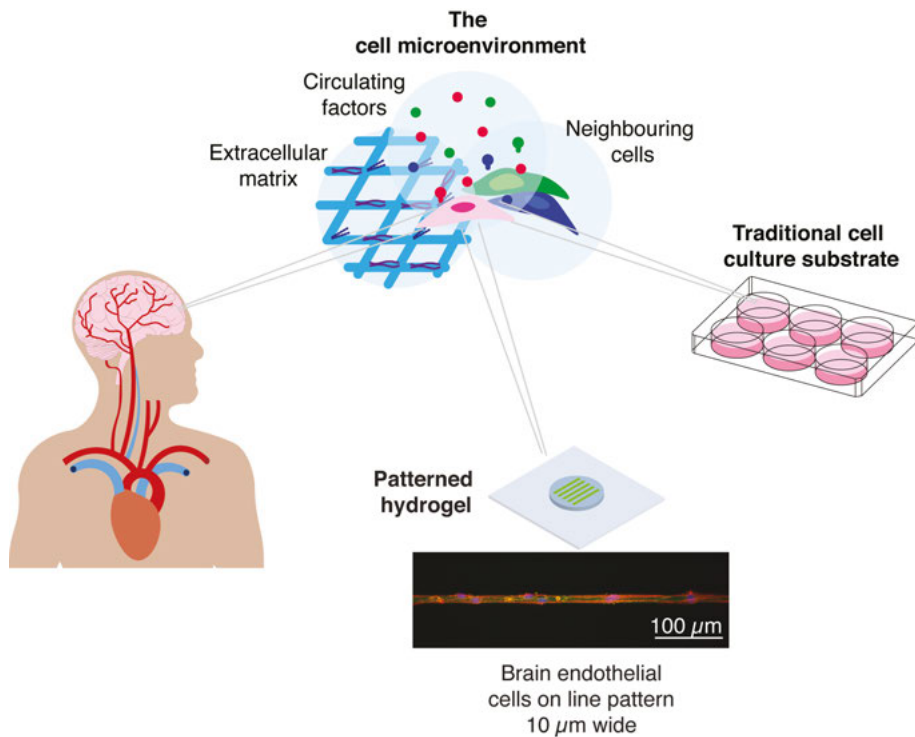


Figure 29. Customized microfluidic chip carrier for the study of brain microvascular endothelial cells. **A.** **B.** Live staining of nuclei (green) and F-actin of brain microvascular endothelial cells inside the microfluidic chip. Scale bar=10 μm **C.** Immunofluorescence of microvascular brain endothelial cells inside of microfluidic chip. Nuclei staining in blue, ZO-1 staining in yellow, F-actin staining in red. Scale bar=10 μm .

Popular Science Summary



The human body consists of a vast number of cells, and jointly, the cells, form tissues and organs. Cells are in contact and communicate with their surroundings, or so-called microenvironment. The cell microenvironment consists partly of the extracellular matrix, a highly hydrated mixture of proteins and polysaccharides where the cells adhere to. Neighbouring cells and circulating biochemical factors also form part of the cell microenvironment. Altogether it gives structural, mechanical, and chemical cues to the cells, dictating their shape and function to form specific tissues.

Biomedical research utilizes *in vitro* models to study the cells' function in health and disease, where cells are grown outside their native tissue. Cells are

grown in a well-controlled artificial environment, that aims to mimic the, the environment that cells experience in the human body (the *in vivo* situation). However, most of the time this is not the case. For example, traditional cell culture substrates, cell culture plates, are almost as stiff as bone, while for example brain and lung tissue are softer than a gummy bear. Furthermore, cell culture plates lack structural cues that guides where and how the cells adhere on these substrates.

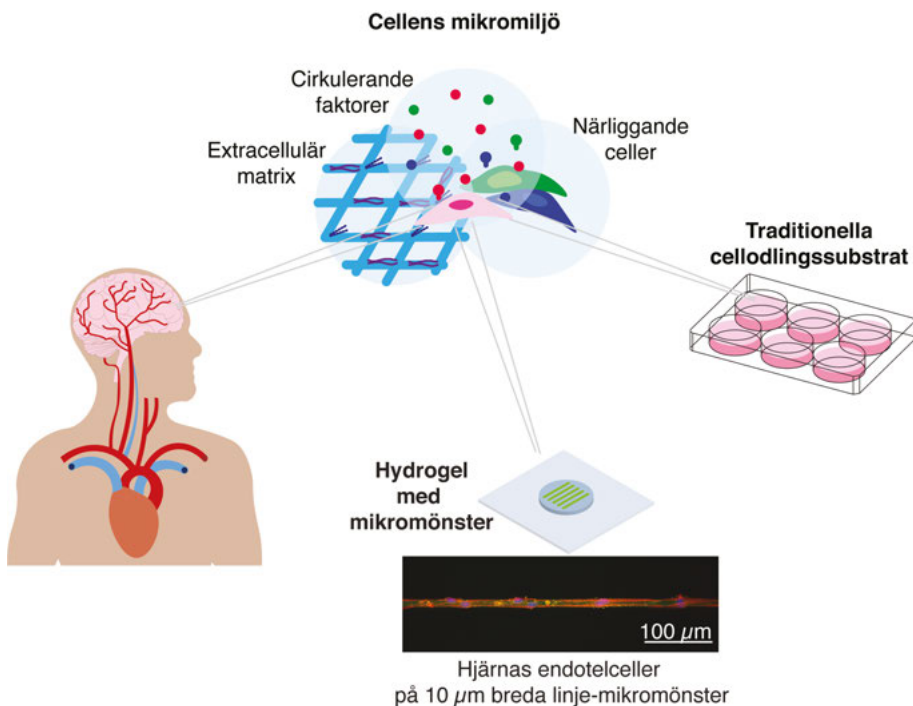
So how can we model this complex environment *in vitro*? How do we study the effect of the microenvironment on the cell? One way is by using hyaluronic acid hydrogels.

In this thesis, first, hyaluronic acid, a polysaccharide found in the extracellular matrix of various tissues, such as the brain, was chemically functionalized to form hydrogels. Hydrogels are an interesting type of materials to be used as cell substrate due to their high-water content that makes them as soft as tissue *in vivo*. Second, the same chemical functionalities were used to control the size and geometry of cells by forming micrometre sized cell adhesive regions, on these hydrogels, or so-called micropatterns. The micropatterns dictate where the cells will adhere, and the cells will adapt their shape to these regions. These hydrogels were then used to study changes of the cell morphology of brain microvascular endothelial cells *in vitro*.

Brain microvascular endothelial cells form the small blood vessels (or microvessels). Microvessels are around 10 μm in diameter, 10 times smaller than the thickness of a strand of hair. These microvessels forms a protective network, also known as the blood brain barrier, that transports oxygen and nutrients to the brain, but also protects it from toxic molecules reaching the brain tissue. Endothelial cells are very small, about 10 to 30 μm in width and they have elongated shape, *i.e.*, they are long and thin. However, under for example disease states, these cells take less elongated shapes and become dysfunctional, causing the vessels to become more permeable, leaving the brain unprotected from toxic molecules.

These cells were cultured on hydrogels to study the how their shape changes. Cells on line micropatterns 10 μm in width, showed a more elongated morphology, compared to cells growing on hydrogels without micropatterns, as cells on cell culture plates. As the cell adhesive area increased to up to 400 μm wide, the cells became less elongated. Also, changes in cell shape were observed when cells were exposed to extreme glucose concentrations, very high or very low, as patients with diabetes would experience. Cells in high and low glucose showed less elongated morphology when growing on 10 μm wide lines. This indicates that the blood brain barrier can become leaky due to extreme glucose levels, causing toxic molecules to reach the brain.

Svensk Sammanfattning



Människokroppen består av ett stort antal celler som tillsammans bildar vävnader och organ. Cellerna är i kontakt, och kommunicerar, med sin omgivning, den så kallade mikromiljön. Cellens mikromiljö består delvis av den extracellulära matrisen, en vattenbaserad blandning av proteiner och polysackarider som cellerna fäster i. Närliggande celler och cirkulerande biokemiska faktorer ingår också i cellmikromiljön. Sammantaget ger den strukturella, mekaniska och kemiska signaler till cellerna, vilket dikterar deras form och funktion för att bilda specifika vävnader.

Biomedicinsk forskning använder *in vitro*-modeller för att studera cellernas funktion i hälsa och sjukdom, där celler odlas utanför sin ursprungliga vävnad. Celler odlas i en välkontrollerad artificiell miljö, som syftar till att efterlikna *in vivo*-miljön, miljön i kroppen. Men för det mesta är skillnaderna stora. Till exempel är traditionella cellodlingssubstrat, cellodlingsplattor, nästan styva

som ben, medan till exempel hjärn- och lungvävnad är mjukare än en gummibjörn. Dessutom saknar cellodlingsplattorna strukturella ledtrådar som styr var och hur cellerna fäster på dessa substrat.

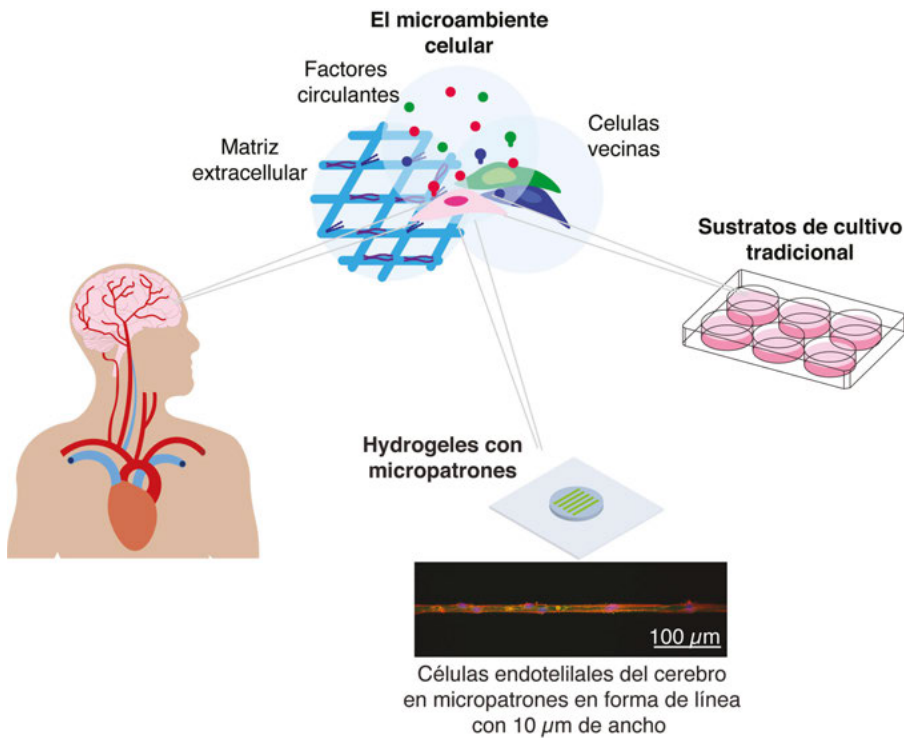
Så hur kan vi modellera denna komplexa miljö in vitro? Hur studerar vi effekten som mikromiljön har på cellen? Ett sätt är att använda hyaluronsyrahydrogeler.

I denna avhandling funktionaliserades först hyaluronsyra, en polysackarid som finns i den extracellulära matrisen i olika vävnader, såsom hjärnan, för att bilda hydrogeler. Hydrogeler är en intressant typ av material att använda som cellsubstrat på grund av deras höga vattenhalt som gör dem lika mjuka som vävnaden in vivo. Dessutom användes samma kemiska funktionalisering för att kontrollera storlek och geometri hos cellerna genom bildandet av mikrometerstora cellregioner på dessa hydrogeler, så kallade mikromönster. Mikromönstren bestämmer var cellerna kommer att fästa, och cellerna kommer att anpassa sin form till dessa regioner. Dessa hydrogeler användes sedan för att studera förändringar av cellmorfologin hos hjärnans mikrovaskulära endotelceller in vitro.

Hjärnans mikrovaskulära endotelceller bildar små blodkärl (eller mikrokärl). Mikrokärl är cirka 10 μm i diameter, 10 gånger mindre än tjockleken på ett hårstrå. Dessa mikrokärl bildar ett skyddande nätverk, även känt som blod-hjärnbarriären, som transporterar syre och näringsämnen till hjärnan, men som också skyddar den från att giftiga molekyler når hjärnvävnaden. Endotelceller är mycket små, cirka 10 till 30 μm breda och de har en långsträckt form, dvs de är långa och tunna. Men under till exempel sjukdomstillstånd antar dessa celler mindre långsträckta former och blir dysfunktionella, vilket gör att kärlen blir mer permeabla, vilket lämnar hjärnan oskyddad från giftiga molekyler.

Dessa celler odlades på hydrogeler för att studera hur deras form förändras. Celler som växte på 10 μm breda linje-mikromönster visade en mer förlängd morfologi, jämfört med celler som växte på hydrogeler utan mikromönster, som celler på cellodlingsplattor. När kontaktytan för cellen ökade till upp till 400 μm bred, blev cellerna mindre förlängda. Dessutom observerades förändringar i cellformen när celler exponerades för extrema glukoskoncentrationer, mycket höga eller mycket låga, som kan uppkomma hos patienter med diabetes. Celler i hög eller låg glukoshalt uppvisade mindre förlängd morfologi när de växte på 10 μm breda linjer. Detta indikerar att blod-hjärnbarriären kan börja läcka på grund av extrema glukosnivåer, vilket gör att giftiga molekyler kan nå hjärnan.

Ciencia Popular



El cuerpo humano está formado por un gran número de células y, en conjunto, las células forman tejidos y órganos. Las células están en contacto y se comunican con su entorno, o el llamado microambiente. El microambiente celular consiste en parte en la matriz extracelular, una mezcla altamente hidratada de proteínas y polisacáridos a la que se adhieren las células. Las células vecinas y los factores bioquímicos circulantes también forman parte del microambiente celular. En conjunto, el microambiente da señales estructurales, mecánicas y químicas a las células, dictando su forma y función para formar tejidos específicos.

La investigación biomédica utiliza modelos *in vitro* para estudiar la función de las células en estados salud y enfermedad, donde las células se cultivan fuera de su tejido nativo. Las células se cultivan en un entorno artificial controlado, que trata de imitar el entorno que las células están expuestas en el cuerpo. Sin embargo, la mayoría de las veces este no es el caso. Por ejemplo, los sustratos de cultivo celular tradicionales, las placas de cultivo celular son casi tan rígidos como el hueso, mientras que, por ejemplo, el tejido cerebral y pulmonar es más suave que un osito de goma. Además, las placas de cultivo celular carecen de señales estructurales que guíen dónde y cómo se adhieren las células a estos sustratos.

Entonces, ¿cómo podemos modelar este entorno complejo *in vitro*? ¿Cómo estudiamos el efecto del microambiente en la célula? Una forma es mediante el uso de hidrogeles de ácido hialurónico.

En esta tesis, primero, el ácido hialurónico, un polisacárido que se encuentra en la matriz extracelular de varios tejidos, como el cerebro, se funcionalizó químicamente para formar hidrogeles. Los hidrogeles son un tipo interesante de materiales para ser utilizados como sustrato celular debido a su alto contenido de agua que los hace tan suaves como el tejido *in vivo*. En segundo lugar, se usaron las mismas funcionalidades químicas para controlar el tamaño y la geometría de las células mediante la formación de regiones adhesivas de células de tamaño micrométrico, o micropatrones. Los micropatrones dictan dónde se adherirán las células, y las células adaptarán su forma a estas regiones. Estos hidrogeles luego se usaron para estudiar los cambios de la morfología celular de las células endoteliales microvasculares del cerebro *in vitro*.

Las células endoteliales microvasculares del cerebro forman los pequeños vasos sanguíneos (o microvasos). Los microvasos tienen alrededor de 10 μm de diámetro, 10 veces más pequeños que el grosor de un mechón de cabello. Estos microvasos forman una red protectora, también conocida como barrera hematoencefálica, que transporta oxígeno y nutrientes al cerebro, pero también lo protege de las moléculas tóxicas que llegan al tejido cerebral. Las células endoteliales son muy pequeñas, de unos 10 a 30 μm de ancho y tienen forma alargada. Sin embargo, bajo estados de enfermedad, por ejemplo, estas células toman formas menos alargadas y se vuelven disfuncionales, lo que hace que los vasos se vuelvan más permeables, dejando al cerebro desprotegido de las moléculas tóxicas.

Estas células se cultivaron en hidrogeles para estudiar cómo cambia su forma. Las células en micropatrones en forma de línea con 10 μm de ancho mostraron una morfología más alargada, en comparación con las células que crecen en hidrogeles sin micropatrones, como células en placas de cultivo celular. A medida que el área adhesiva de las células aumentaba hasta 400 μm de ancho,

las células se alargaban menos. Además, se observaron cambios en la forma de las células cuando las células se expusieron a concentraciones extremas de glucosa, muy altas o muy bajas, como las que experimentarían los pacientes con diabetes. Las células en glucosa alta y baja mostraron una morfología menos alargada cuando crecieron en líneas de 10 μm de ancho. Esto indica que la barrera hematoencefálica puede tener fugas debido a los niveles extremos de glucosa, lo que causaría que moléculas tóxicas lleguen al cerebro.

Acknowledgements

I would like to start thanking my supervisors. Maria Tenje thank you for taking me Exploring Microsystems Technologies for Life Science Applications, it's been a ride! Thank you for your supervision. Maria Antfolk, thank you for joining as co-supervisor. Thank you for all your supervision, help and for always being available for a quick zoom call. Thank you both for teachings to become a better researcher. It was so special to have had two women as supervisors.

I am so grateful to all EMBLA group members, previous and current. The EMBLA group will always have a special place in my heart. This group has been so much fun to work with, filled with great women scientist and international members making it extra special, all of you have been so kind and helpful through these years. Hannah Pohlit, thank you for your short co-supervision, discussions, help in the lab, contributions to the papers and good times. Laurent Barbe, thank you for your contributions to the papers, the long chats (about science, dogs, and ski) and all your help and support in the labs. Thank you Cantoni, for collaborating with me, taking care of the cell lab, all the hydrogel discussions, sharing the confocal with me, and for always being there to help. Sarah, the best office neighbour I could have asked for. Thank you for always being there to discuss science and other no so scientific topics, thank you for taking care of the cell lab, all the coffees and padel matches. Gabriel, thank you for your help discussing and fixing my little, annoying, and sometimes silly problems with Excel, image analysis, cutter plotter, or in finding ways how to storage my samples; and for being silly with me at work. Susan thank you for ALL you do and cheering me up with your fun and bubbly personality. Atena, thank you for sharing the confocal with me and always taking the time to talk. Thank you, Sofia, for your supervision and feedback writing the review. Thank you Samah, for always being there for a chat. Quian thank you for your kindness and always sharing Chinese gifts. Zhenhua, thank you for always being there when I needed help after 19 on slack. Thanks to the far away and newer EMBLA members Yuan, Praneeth and Sagar for your contributions to the group. Thanks to previous members, Anna Kim, Milena, Martin A, for always being there to help or just to talk. Big thanks to the first EMBLA generation, Frida Sjögren, thank you for supervising my master's thesis project in the group, introducing me to microfabricated hydrogels and all the

coffees. Thank you, Gemma Mestres for introducing me to cell culture of adherent mammalian cells and your Spanish energy that you brought to the group. Thank you, Anette Wolff for introducing me to the world of BBB and microfabricated *in vitro* models. Thanks to Mathias Ohlin, Anna Fornell for all your input to the group. Sean for your contributions to the EMBLA group, but mostly for our long friendship. Also, I want to thank to the honorary members of the EMBLA group. First, thank you Daniel Feldt for contributing into exploring microcontact printing of HA hydrogels, you were such a good and independent student. Björn and Samuel, thank for being so funny, it was nice to have you guys around. Mara, thank you for sharing your knowledge, protocols, and occludin abs during your visit to our lab, it was so much fun to share the lab with you. Noelia, thank you for visiting us from so far away, it was so nice to share labs, knowledge, and yoga with you.

Big thanks to all the people from MST for introducing me to the microfabrication world. Lena thank you for ALL you have done for the division, keeping the labs running, answering all my statistics and MNTI questions, and your delicious fika. Thank you, Hugo Nyugen, for your technical help in drawing and printing my masks and 3D-printing my UV lamp holder. Thank you, Jan, for taking care of the chemi lab and for being your calm self. Javier Cruz thank you for always being there ready to help. Karolina Svenson, thank you for always being there to listen. Simon Sodergren, thank you for being so kind and making sure no fika goes to waste. Bei, thank you for being a lab buddy in the clean room outside working hours. Klara, thank you for your time in MST and my beanie. Thank you Klas for being such a fun head of division.

Thanks to MSL for keeping the clean room running. Special thanks to Rimantas, thank you for sharing your knowledge on lithography, talking to you really helped my project. Thank you, Sven, for always bringing my ethanol and taking care of all my chemical waste. Thank you Örjan for always being there to help, answer questions, printing emergency masks or just to chat.

Finally, thanks to all the building neighbours that I get to meet and collaborate with. Thanks to Dmitri Ossipov for introducing me to hyaluronic acid hydrogels and his supervision. Thank you, Sergey Rodin for our short collaboration and always be there for questions or a chat. Thank you Jörgen for all your help and support to finish my studies. Anna Blassi, thank you for your body combat classes and helping me find media. Thank you, corridor neighbours, Sussanne, Camila and Amina for the fikas.

But there is also so many people from not so academic world that I would like to thank. Chris B thank you for your teachings and sharing the yoga practice. Thank you, Kayleigh, for your trainings, teachings, good chats and laughs. A

big shout out to all the people who might not have been in the lab with me or seen me every day or barely text once a month, but I want to thank you for the fun times we shared to help me through this: Amy, Iohan, Viviana, Anaëlle, Jean, Callie, Johan, Andreas, Maxim, Frida N, Emilie Å, Adam Å and Albert Å. Special thanks to Anja and Ingvar Åberg, thank you for welcoming to your family, thank you for the Swedish and ski lessons, travels, delicious food and all your cheering and support.

Big thanks to the one person who saw me every day through this process, Simon Åberg, thank you so much for everything you have done (it is a very long list). I would have not been able to do this without you.

Finally, I would like to thank my family, for all the love, support, and fun times together. Thank you, dad, for all your love and support since ever, thank you for really everything you have done for me (big list here too). Thank you, mom, for always worrying about me. Both of you always had my back and pushed me to be my best self, and everything I have done is thanks to you. Finally, thanks to my brother and sister, Tali and Viki, you were both like a second set of parents. All of you have been great models of hard work and perseverance.

References

1. Sun Y, Chen CS, Fu J. Forcing stem cells to behave: A biophysical perspective of the cellular microenvironment. *Annu Rev Biophys.* 2012;41(1):519–42.
2. Romani P, Valcarcel-Jimenez L, Frezza C, Dupont S. Crosstalk between mechanotransduction and metabolism. *Nat Rev Mol Cell Biol.* 2021;22(1):22–38.
3. Peppas NA, Hilt JZ, Khademhosseini A, Langer R. Hydrogels in biology and medicine: From molecular principles to bionanotechnology. *Adv Mater.* 2006;18(11):1345–60.
4. Thiele J, Ma Y, Bruckers SMC, Ma S, Huck WTS. 25th anniversary article: Designer hydrogels for cell cultures: A materials selection guide. Vol. 26, *Advanced Materials*. John Wiley & Sons, Ltd; 2014. p. 125–48.
5. Tenje M, Cantoni F, Porras Hernández AM, Searle SS, Johansson S, Barbe L, et al. A practical guide to microfabrication and patterning of hydrogels for biomimetic cell culture scaffolds. *Organs-on-a-Chip.* 2020;2(January):100003.
6. Voldman J, Gray ML, Schmidt MA. Microfabrication in biology and medicine. *Annu Rev Biomed Eng.* 1999;(1):401–25.
7. Folch A. Introduction to BioMEMS. *Introduction to BioMEMS.* 2013.
8. Théry M. Micropatterning as a tool to decipher cell morphogenesis and functions. Vol. 123, *Journal of Cell Science.* 2010. p. 4201–13.
9. Annabi N, Tamayol A, Uquillas JA, Akbari M, Bertassoni LE, Cha C, et al. 25th anniversary article: Rational design and applications of hydrogels in regenerative medicine. *Adv Mater.* 2014;26(1):85–124.
10. Chen CS, Mrksich M, Huang S, Whitesides GM, Ingber DE. Geometric control of cell life and death. *Science (80-).* 1997 May 30;276(5317):1425–8.
11. Wan LQ, Ronaldson K, Park M, Taylor G, Zhang Y, Gimble JM, et al. Micropatterned mammalian cells exhibit phenotype-specific left-right asymmetry. *Proc Natl Acad Sci U S A.* 2011;108(30):12295–300.
12. Aird WC. Endothelial cell heterogeneity. *Cold Spring Harb Perspect Med.* 2012;2(1):1–14.
13. Daneman R, Prat A. The blood-brain barrier. *Cold Spring Harb Perspect Biol.* 2015 Jan;7(1):a020412.
14. Mahringer A, Ott M, Fricker G. The Blood–Brain Barrier: An Introduction to Its Structure and Function BT - The Blood Brain Barrier (BBB). In: Fricker G, Ott M, Mahringer A, editors. Berlin, Heidelberg: Springer Berlin Heidelberg; 2014. p. 1–20.
15. Abbott NJ, Patabendige AAK, Dolman DEM, Yusof SR, Begley DJ. Structure and function of the blood-brain barrier. *Neurobiol Dis.* 2010;37(1):13–25.

16. Frantz C, Stewart KM, Weaver VM. The extracellular matrix at a glance. *J Cell Sci.* 2010;123(24):4195–200.
17. Miyake K, Satomi N, Sasaki S. Elastic modulus of polystyrene film from near surface to bulk measured by nanoindentation using atomic force microscopy. *Appl Phys Lett.* 2006;89(3).
18. Discher DE, Janmey P, Wang Y. Tissue Cells Feel and Respond to the Stiffness of Their Substrate. *Mater Biol.* 2005;310(NOVEMBER):1139–43.
19. Guimarães CF, Gasperini L, Marques AP, Reis RL. The stiffness of living tissues and its implications for tissue engineering. *Nat Rev Mater.* 2020;5(5):351–70.
20. Williams SH, Wright BW, Den Truong V, Daubert CR, Vinyard C. Mechanical Properties of Foods Used in Experimental Studies of Primate Masticatory Function. *Am J Primatol.* 2005;67:329–46.
21. Caliri SR, Burdick JA. A practical guide to hydrogels for cell culture. *Nat Methods.* 2016;13(5):405–14.
22. Lutolf MP, Hubbell JA. Synthetic biomaterials as instructive extracellular microenvironments for morphogenesis in tissue engineering [Internet]. Vol. 23, *Nature Biotechnology*. Nature Publishing Group; 2005 [cited 2019 Oct 9]. p. 47–55. Available from: <http://www.nature.com/articles/nbt1055>
23. Lam J, Truong NF, Segura T. Design of cell-matrix interactions in hyaluronic acid hydrogel scaffolds. *Acta Biomater.* 2014;10(4):1571–80.
24. Bignami A, Hosley M, Dahl D. Hyaluronic acid and hyaluronic acid-binding proteins in brain extracellular matrix. Vol. 188, *Anatomy and Embryology*. Springer-Verlag; 1993. p. 419–33.
25. Amorim S, Reis CA, Reis RL, Pires RA. Extracellular Matrix Mimics Using Hyaluronan-Based Biomaterials. *Trends Biotechnol* [Internet]. 2021;39(1):90–104.
26. Fraser JRE, Laurent TC, Laurent UBG. Hyaluronan: Its nature, distribution, functions and turnover. *J Intern Med.* 1997;242(1):27–33.
27. Girish KS, Kemparaju K. The magic glue hyaluronan and its eraser hyaluronidase: A biological overview. *Life Sci.* 2007;80(21):1921–43.
28. Yang C, Cao M, Liu H, He Y, Xu J, Du Y, et al. The high and low molecular weight forms of hyaluronan have distinct effects on CD44 clustering. *J Biol Chem.* 2012;287(51):43094–107.
29. Kouvidi K, Berdiaki A, Nikitovic D, Katonis P, Afratis N, Hascall VC, et al. Role of Receptor for Hyaluronic Acid-mediated Motility (RHAMM) in Low Molecular Weight Hyaluronan (LMWHA)- mediated fibrosarcoma cell adhesion. *J Biol Chem.* 2011;286(44):38509–20.
30. Collins MN, Birkinshaw C. Hyaluronic acid based scaffolds for tissue engineering - A review. *Carbohydr Polym.* 2013;92(2):1262–79.
31. Vega SL, Kwon MY, Song KH, Wang C, Mauck RL, Han L, et al. Combinatorial hydrogels with biochemical gradients for screening 3D cellular microenvironments. *Nat Commun.* 2018 Dec 9 [cited 2019 May 27];9(1):614.
32. Marklein RA, Burdick JA. Spatially controlled hydrogel mechanics to modulate stem cell interactions. *Soft Matter.* 2009;6(1):136–43.
33. Duan B, Yin Z, Hockaday Kang L, Magin RL, Butcher JT. Active tissue stiffness modulation controls valve interstitial cell phenotype and osteogenic potential in 3D culture. *Acta Biomater.* 2016 May 1;36:42–54.
34. Lampi MC, Guvendiren M, Burdick JA, Reinhart-King CA. Photopatterned

- Hydrogels to Investigate the Endothelial Cell Response to Matrix Stiffness Heterogeneity. *ACS Biomater Sci Eng*. 2017 Nov 13;3(11):3007–16.
35. Wu S, Xu R, Duan B, Jiang P. Three-dimensional hyaluronic acid hydrogel-based models for in vitro human iPSC-derived NPC culture and differentiation. *J Mater Chem B*. 2017 May 31;5(21):3870–8.
 36. Shi L, Wang F, Zhu W, Xu Z, Fuchs S, Hilborn J, et al. Self-Healing Silk Fibroin-Based Hydrogel for Bone Regeneration: Dynamic Metal-Ligand Self-Assembly Approach. *Adv Funct Mater*. 2017 Oct 5;27(37).
 37. Choi JR, Yong KW, Choi JY, Cowie AC. Recent advances in photocrosslinkable hydrogels for biomedical applications. *Biotechniques*. 2019 Jan [cited 2019 May 9];66(1):40–53.
 38. Kamoun EA, El-Betany A, Menzel H, Chen X. Influence of photoinitiator concentration and irradiation time on the crosslinking performance of visible-light activated pullulan-HEMA hydrogels. *Int J Biol Macromol*. 2018;120:1884–92.
 39. Oyen ML. Mechanical characterisation of hydrogel materials. *Int Mater Rev*. 2014;59(1):44–59.
 40. Lin DC, Horkay F. Nanomechanics of polymer gels and biological tissues: A critical review of analytical approaches in the Hertzian regime and beyond. *Soft Matter*. 2008;4(4):669–82.
 41. Chen Z, Lee JB. Biocompatibility of su-8 and its biomedical device applications. *Micromachines*. 2021;12(7).
 42. Liu VA, Bhatia SN. Three-Dimensional Photopatterning of Hydrogels Containing Living Cells. *Biomed Microdevices*. 2002;4(4):257–66.
 43. Seo JH, Shin DS, Mukundan P, Revzin A. Attachment of hydrogel microstructures and proteins to glass via thiol-terminated silanes. *Colloids Surfaces B Biointerfaces*. 2012 Oct 1;98:1–6.
 44. Ratner BD, Hoffman AS, McArthur SL. *Physicochemical Surface Modification of Materials Used in Medicine*. Fourth Edi. Biomaterials Science. Elsevier; 2020. 487–505 p.
 45. Curtis ASG, Forrester J V., McInnes C, Lawrie F. Adhesion of cells to polystyrene surfaces. *J Cell Biol*. 1983;97(5 I):1500–6.
 46. Lerman MJ, Lembong J, Muramoto S, Gillen G, Fisher JP. The Evolution of Polystyrene as a Cell Culture Material. *Tissue Eng - Part B Rev*. 2018;24(5):359–72.
 47. Goodman SR. Cell Adhesion and the Extracellular Matrix. In: Goodman SR, editor. *Goodman's Medical Cell Biology*. 4th ed. Elsevier; 2021. p. 203–47.
 48. Barczyk M, Carracedo S. Integrins. *Cell Tissue Res*. 2010 Jan 20 [cited 2019 Oct 8];339(1):269–80.
 49. Humphries JD, Byron A, Humphries MJ. Integrin ligands at a glance. *J Cell Sci*. 2006;119(19):3901–3.
 50. Gegenfurtner FA, Jahn B, Wagner H, Ziegenhain C, Enard W, Geistlinger L, et al. Micropatterning as a tool to identify regulatory triggers and kinetics of actin-mediated endothelial mechanosensing. *J Cell Sci*. 2018;131(10).
 51. Chen CS, Mrksich M, Huang S, Whitesides GM, Ingber DE. Micropatterned surfaces for control of cell shape, position, and function. *Biotechnol Prog* [Internet]. 1998 Jun 5 [cited 2019 Jul 29];14(3):356–63. Available from: <http://doi.wiley.com/10.1021/bp980031m>
 52. Castaño AG, Hortigüela V, Lagunas A, Cortina C, Montserrat N, Samitier J,

- et al. Protein patterning on hydrogels by direct microcontact printing: Application to cardiac differentiation. *RSC Adv.* 2014 Jul 4;4(55):29120–3.
53. Hsiao TW, Tresco PA, Hlady V. Astrocytes alignment and reactivity on collagen hydrogels patterned with ECM proteins. *Biomaterials.* 2015 Jan [cited 2018 Sep 26];39:124–30.
 54. Hahn MS, Taite LJ, Moon JJ, Rowland MC, Ruffino KA, West JL. Photolithographic patterning of polyethylene glycol hydrogels. *Biomaterials.* 2006 Apr;27(12):2519–24.
 55. Kharkar PM, Rehmann MS, Skeens KM, Maverakis E, Kloxin AM. Thiol-ene Click Hydrogels for Therapeutic Delivery. *ACS Biomater Sci Eng.* 2016;2(2):165–79.
 56. Anderson DEJ, Hinds MT. Endothelial cell micropatterning: Methods, effects, and applications. *Ann Biomed Eng.* 2011 Sep 15;39(9):2329–45.
 57. Aird WC. Phenotypic heterogeneity of the endothelium: I. Structure, function, and mechanisms. *Circ Res.* 2007;100(2):158–73.
 58. Aird WC. Phenotypic heterogeneity of the endothelium: II. Representative vascular beds. *Circ Res.* 2007;100(2):174–90.
 59. Gray KM, Stroka KM. Vascular endothelial cell mechanosensing: New insights gained from biomimetic microfluidic models. *Semin Cell Dev Biol.* 2017;71:106–17.
 60. Wong AD, Ye M, Levy AF, Rothstein JD, Bergles DE, Searson PC. The blood-brain barrier: An engineering perspective. Vol. 6, *Frontiers in Neuroengineering.* Front Neuroeng; 2013
 61. Sandoval KE, Witt KA. Blood-brain barrier tight junction permeability and ischemic stroke. *Neurobiol Dis.* 2008;32(2):200–19.
 62. Rahman NA, Rasil ANHM, Meyding-Lamade U, Craemer EM, Diah S, Tuah AA, et al. Immortalized endothelial cell lines for in vitro blood–brain barrier models: A systematic review. *Brain Res.* 2016 Jul;1642:532–45.
 63. Takahashi K, Tanabe K, Ohnuki M, Narita M, Ichisaka T, Tomoda K, et al. Induction of Pluripotent Stem Cells from Adult Human Fibroblasts by Defined Factors. *Cell.* 2007;131(5):861–72.
 64. Lippmann ES, Al-Ahmad A, Palecek SP, Shusta E V. Modeling the blood-brain barrier using stem cell sources. *Fluids Barriers CNS.* 2013;10(1):1–14.
 65. Brown RC, Morris AP, O’Neil RG. Tight junction protein expression and barrier properties of immortalized mouse brain microvessel endothelial cells. *Brain Res.* 2007 Jan;1130(1):17–30.
 66. Eigenmann DE, Xue G, Kim KS, Moses A V., Hamburger M, Oufir M. Comparative study of four immortalized human brain capillary endothelial cell lines, hCMEC/D3, hBMEC, TY10, and BB19, and optimization of culture conditions, for an in vitro blood-brain barrier model for drug permeability studies. *Fluids Barriers CNS.* 2013;10(1).
 67. Sivandzade F, Cucullo L. In-vitro blood–brain barrier modeling: A review of modern and fast-advancing technologies. *J Cereb Blood Flow Metab.* 2018;38(10):1667–81.
 68. Kapitulnik J, Benaim C, Sasson S. Endothelial Cells Derived from the Blood-Brain Barrier and Islets of Langerhans Differ in their Response to the Effects of Bilirubin on Oxidative Stress Under Hyperglycemic Conditions . Vol. 3, *Frontiers in Pharmacology* . 2012. p. 131.
 69. Yan J, Zhang Z, Shi H. HIF-1 is involved in high glucose-induced paracellular

- permeability of brain endothelial cells. *Cell Mol Life Sci*. 2012 Jan 27 ;69(1):115–28.
70. Wang Z, Chen GQ, Yu GP, Liu CJ. Pyrroloquinoline quinone protects mouse brain endothelial cells from high glucose-induced damage in vitro. *Acta Pharmacol Sin*. 2014;35(11):1402–10.
 71. Kemeny SF, Figueroa DS, Clyne AM. Hypo- and Hyperglycemia Impair Endothelial Cell Actin Alignment and Nitric Oxide Synthase Activation in Response to Shear Stress. *PLoS One*. 2013;8(6).
 72. Sajja RK, Prasad S, Cucullo L. Impact of altered glycaemia on blood-brain barrier endothelium: An in vitro study using the hCMEC/D3 cell line. *Fluids Barriers CNS*. 2014 Apr 5;11(1):8.
 73. Zhao F, Deng J, Yu X, Li D, Shi H, Zhao Y. Protective effects of vascular endothelial growth factor in cultured brain endothelial cells against hypoglycemia. *Metab Brain Dis*. 2015 Aug 13;30(4):999–1007.
 74. Bogush M, Heldt NA, Persidsky Y. Blood Brain Barrier Injury in Diabetes: Unrecognized Effects on Brain and Cognition. *J Neuroimmune Pharmacol*. 2017;12(4):593–601.
 75. Prasad S, Sajja RK, Naik P, Cucullo L. Diabetes Mellitus and Blood-Brain Barrier Dysfunction: An Overview. *J Pharmacovigil*. 2014;02(02).
 76. Barrett EJ, Liu Z, Khamaisi M, King GL, Klein R, Klein BEK, et al. Diabetic microvascular disease: An endocrine society scientific statement. *J Clin Endocrinol Metab*. 2017;102(12):4343–410.
 77. Hahn C, Schwartz MA. Mechanotransduction in vascular physiology and atherogenesis. *Nat Rev Mol Cell Biol*. 2009;10(1):53–62.
 78. van der Meer AD, Poot AA, Feijen J, Vermes I. Analyzing shear stress-induced alignment of actin filaments in endothelial cells with a microfluidic assay. *Biomicrofluidics*. 2010;4(1).
 79. Tkachenko E, Gutierrez E, Saikin SK, Fogelstrand P, Kim C, Groisman A, et al. The nucleus of endothelial cell as a sensor of blood flow direction. *Biol Open*. 2013;2(10):1007–12.
 80. Reinitz A, DeStefano J, Ye M, Wong AD, Searson PC. Human brain microvascular endothelial cells resist elongation due to shear stress. *Microvasc Res*. 2015 May 1;99:8–18.
 81. DeStefano JG, Xu ZS, Williams AJ, Yimam N, Searson PC. Effect of shear stress on iPSC-derived human brain microvascular endothelial cells (dhBMECs). *Fluids Barriers CNS*. 2017 Aug 4;14(1).
 82. Brower JB, Targovnik JH, Bowen BP, Caplan MR, Massia SP. Elevated glucose impairs the endothelial cell response to shear stress. In: *Cellular and Molecular Bioengineering*. 2009. p. 533–43.
 83. Vartanian KB, Kirkpatrick SJ, Hanson SR, Hinds MT. Endothelial cell cytoskeletal alignment independent of fluid shear stress on micropatterned surfaces. *Biochem Biophys Res Commun*. 2008 Jul;371(4):787–92.
 84. Leslie-Barbick JE, Shen C, Chen C, West JL. Micron-Scale Spatially Patterned, Covalently Immobilized Vascular Endothelial Growth Factor on Hydrogels Accelerates Endothelial Tubulogenesis and Increases Cellular Angiogenic Responses. *Tissue Eng Part A*. 2010;17(1–2):221–9.
 85. Lei Y, Zouani OF, Rémy M, Ayela C, Durrieu M-C. Geometrical Microfeature Cues for Directing Tubulogenesis of Endothelial Cells. *Gerecht S, editor. PLoS One*. 2012 Jul 19;7(7):e41163.

86. Vartanian KB, Berny MA, McCarty OJT, Hanson SR, Hinds MT. Cytoskeletal structure regulates endothelial cell immunogenicity independent of fluid shear stress. *Am J Physiol - Cell Physiol*. 2010;298(2):333–41.
87. Versaev M, Grevesse T, Gabriele S. Spatial coordination between cell and nuclear shape within micropatterned endothelial cells. *Nat Commun*. 2012 Jan;3(1):671.
88. Dike LE, Chen CS, Mrksich M, Tien J, Whitesides GM, Ingber DE. Geometric control of switching between growth, apoptosis, and differentiation during angiogenesis using micropatterned substrates. *Vitr Cell Dev Biol - Anim*. 1999;35(8):441–8.
89. Moon JJ, Hahn MS, Kim I, Nsiah BA, West JL. Micropatterning of poly(ethylene glycol) diacrylate hydrogels with biomolecules to regulate and guide endothelial morphogenesis. *Tissue Eng - Part A*. 2009 Mar 15 [cited 2019 May 28];15(3):579–85.
90. Fukuhara S, Sakurai A, Sano H, Yamagishi A, Somekawa S, Takakura N, et al. Cyclic AMP Potentiates Vascular Endothelial Cadherin-Mediated Cell-Cell Contact To Enhance Endothelial Barrier Function through an Epac-Rap1 Signaling Pathway. *Mol Cell Biol*. 2005;25(1):136–46.
91. O'Connor BB, Grevesse T, Zimmerman JF, Ardoña HAM, Jimenez JA, Bitounis D, et al. Human brain microvascular endothelial cell pairs model tissue-level blood-brain barrier function. *Integr Biol (Camb)*. 2020;12(3):64–79.
92. Versaev M, Grevesse T, Gabriele S. Spatial coordination between cell and nuclear shape within micropatterned endothelial cells. *Nat Commun* [Internet]. 2012 Jan 14;3(1):671.
93. Inaki M, Liu J, Matsuno K. Cell chirality: Its origin and roles in left-right asymmetric development. *Philos Trans R Soc B Biol Sci*. 2016;371(1710).
94. Li R, Bowerman B. Symmetry breaking in biology. *Cold Spring Harb Perspect Biol*. 2010;2(3):1–6.
95. Levin M. Left-right asymmetry in embryonic development: A comprehensive review. *Mech Dev*. 2005;122(1):3–25.
96. Palmer AR. What determines direction of asymmetry: Genes, environment or chance? *Philos Trans R Soc B Biol Sci*. 2016;371(1710).
97. Aw S, Levin M. Is left-right asymmetry a form of planar cell polarity? *Development*. 2009;136(3):355–66.
98. Palmer AR. Symmetry breaking and the evolution of development. *Science* (80-). 2004;306(5697):828–33.
99. Raya Á, Izpisua Belmonte JC. Left-right asymmetry in the vertebrate embryo: From early information to higher-level integration. *Nat Rev Genet*. 2006;7(4):283–93.
100. Vandenberg LN, Levin M. A unified model for left-right asymmetry? Comparison and synthesis of molecular models of embryonic laterality. *Dev Biol*. 2013;379(1):1–15.
101. Brown NA, Wolpert L. The development of handedness in left/right asymmetry. *Development*. 1990;109(1):1–9.
102. Inaki M, Sasamura T, Matsuno K. Cell chirality drives left-right asymmetric morphogenesis. *Front Cell Dev Biol*. 2018;6(APR):1–9.
103. Wan LQ, Ronaldson K, Guirguis M, Vunjak-Novakovic G. Micropatterning of cells reveals chiral morphogenesis. *Stem Cell Res Ther*. 2013;4(2).

104. Wan LQ, Chin AS, Worley KE, Ray P. Cell chirality: Emergence of asymmetry from cell culture. *Philos Trans R Soc B Biol Sci.* 2016;371(1710).
105. Yao X, Wang X, Ding J. Exploration of possible cell chirality using material techniques of surface patterning. *Acta Biomater.* 2021;126:92–108.
106. Rahman T, Zhang H, Fan J, Wan LQ. Cell chirality in cardiovascular development and disease. *APL Bioeng.* 2020;4(3).
107. Tee YH, Shemesh T, Thiagarajan V, Hariadi RF, Anderson KL, Page C, et al. Cellular chirality arising from the self-organization of the actin cytoskeleton. *Nat Cell Biol.* 2015;17(4):445–57.
108. Raymond MJ, Ray P, Kaur G, Singh A V., Wan LQ. Cellular and Nuclear Alignment Analysis for Determining Epithelial Cell Chirality. *Ann Biomed Eng.* 2016;44(5):1475–86.
109. Kwong HK, Huang Y, Bao Y, Lam ML, Chen TH. Remnant Effects of Culture Density on Cell Chirality after Reseeding. *ACS Biomater Sci Eng.* 2019;5(8):3944–53.
110. Zhu N, Kwong HK, Bao Y, Chen TH. Chiral orientation of skeletal muscle cells requires rigid substrate. *Micromachines.* 2017;8(6):1–11.
111. Fan J, Ray P, Lu Y, Kaur G, Schwarz JJ, Wan LQ. Cell chirality regulates intercellular junctions and endothelial permeability. *Sci Adv.* 2018;4(10).
112. Das A, Adhikary S, Chowdhury AR, Barui A. Substrate-dependent control of the chiral orientation of mesenchymal stem cells: image-based quantitative profiling. *Biomed Mater.* 2021;16(3).
113. Chen TH, Hsu JJ, Zhao X, Guo C, Wong MN, Huang Y, et al. Left-right symmetry breaking in tissue morphogenesis via cytoskeletal mechanics. *Circ Res.* 2012;110(4):551–9.
114. Worley KE, Shieh D, Wan LQ. Inhibition of cell-cell adhesion impairs directional epithelial migration on micropatterned surfaces. *Integr Biol.* 2015;7(5):580–90.
115. Wan LQ, Vunjak-Novakovic G. Micropatterning chiral morphogenesis. *Commun Integr Biol.* 2011;4(6):745–8.
116. Carpenter AE, Jones TR, Lamprecht MR, Clarke C, Kang IH, Friman O, et al. CellProfiler: Image analysis software for identifying and quantifying cell phenotypes. *Genome Biol.* 2006;7(10).
117. Measure properties of image regions - MATLAB regionprops - MathWorks Nordic.
118. Xu J, Van Keymeulen A, Wakida NM, Carlton P, Berns MW, Bourne HR. Polarity reveals intrinsic cell chirality. *Proc Natl Acad Sci U S A.* 2007;104(22):9296–300.
119. Fan J, Zhang H, Rahman T, Stanton DN, Wan LQ. Cell organelle-based analysis of cell chirality. *Commun Integr Biol.* 2019;12(1):78–81.
120. Zhang H, Fan J, Zhao Z, Wang C, Wan LQ. Effects of Alzheimer's Disease-Related Proteins on the Chirality of Brain Endothelial Cells. *Cell Mol Bioeng.* 2021;14(3):231–40.
121. Singh A V., Mehta KK, Worley K, Dordick JS, Kane RS, Wan LQ. Carbon nanotube-induced loss of multicellular chirality on micropatterned substrate is mediated by oxidative stress. *ACS Nano.* 2014;8(3):2196–205.
122. Zhang H, Wan LQ. Cell Chirality as a Novel Measure for Cytotoxicity. *Adv Biol.* 2022;6(1):1–10.
123. Hempel A, Maasch C, Heintze U, Lindschau C, Dietz R, Luft FC, et al. High

- Glucose Concentrations Increase Endothelial Cell Permeability via Activation of Protein Kinase α . *Circ Res*. 1997 Sep;81(3):363–71.
124. Joshi S, Yu D. Immunofluorescence. *Basic Science Methods for Clinical Researchers*. Elsevier Inc.; 2017. 135–150 p.
 125. Im K, Mareninov S, Palma Diaz FM, Yong W. An Introduction to Performing Immunofluorescence Staining. In: Yong WH, editor. *Biobanking*. Springer; 2018. p. 299–311.
 126. Donaldson JG. Immunofluorescence Staining. *Curr Protoc Cell Biol*. 2015;69(1):4.3.1-4.3.7.
 127. Smith CL. Basic confocal microscopy. *Curr Protoc Mol Biol*. 2008;(SUPPL. 81):1–18.
 128. Chen W, Li W, Dong X, Pei J. A Review of Biological Image Analysis. *Curr Bioinform*. 2018;13(4):337–43.
 129. Schneider CA, Rasband WS, Eliceiri KW. NIH Image to ImageJ: 25 years of image analysis. *Nat Methods*. 2012;9(7):671–5.
 130. Gonzalez RC, Woods RE. *Digital Image Analysis*. Adison-Wesleu Publishing Company Inc.; 1993.
 131. Rocha L, Velho L, Carvalho PCP. Image moments-based structuring and tracking of objects. *Brazilian Symp Comput Graph Image Process*. 2002;2002-Janua(1):99–105.

Acta Universitatis Upsaliensis

*Digital Comprehensive Summaries of Uppsala Dissertations
from the Faculty of Science and Technology 2153*

Editor: The Dean of the Faculty of Science and Technology

A doctoral dissertation from the Faculty of Science and Technology, Uppsala University, is usually a summary of a number of papers. A few copies of the complete dissertation are kept at major Swedish research libraries, while the summary alone is distributed internationally through the series Digital Comprehensive Summaries of Uppsala Dissertations from the Faculty of Science and Technology. (Prior to January, 2005, the series was published under the title "Comprehensive Summaries of Uppsala Dissertations from the Faculty of Science and Technology".)



ACTA
UNIVERSITATIS
UPSALIENSIS
UPPSALA
2022

Distribution: publications.uu.se
urn:nbn:se:uu:diva-473037